Fraunhofer
ITWM

M. Taralov, V. Taralova, P. Popov, O. Iliev, A. Latz,
J. Zausch

Report on Finite Element Simulations of Electrochemical Processes in Li-ion Batteries with Thermic Effects

Berichte des Fraunhofer ITWM, Nr. 221 (2012)

ISSN 1434-9973

Bericht 221 (2012)

Die Veröffentlichungen in der Berichtsreihe des Fraunhofer ITWM können bezogen werden über:

Fraunhofer-Institut für Techno- und
Wirtschaftsmathematik ITWM
Fraunhofer-Platz 1

67663 Kaiserslautern
Germany

Telefon: +49(0)631/31600-4674
Telefax: +49(0)631/31600-5674
E-Mail: presse@itwm.fraunhofer.de
Internet: www.itwm.fraunhofer.de

Vorwort

Das Tätigkeitsfeld des Fraunhofer-Instituts für Techno- und Wirtschaftsmathematik ITWM umfasst anwendungsnahe Grundlagenforschung, angewandte Forschung sowie Beratung und kundenspezifische Lösungen auf allen Gebieten, die für Techno- und Wirtschaftsmathematik bedeutsam sind.

In der Reihe »Berichte des Fraunhofer ITWM« soll die Arbeit des Instituts kontinuierlich einer interessierten Öffentlichkeit in Industrie, Wirtschaft und Wissenschaft vorgestellt werden. Durch die enge Verzahnung mit dem Fachbereich Mathematik der Universität Kaiserslautern sowie durch zahlreiche Kooperationen mit internationalen Institutionen und Hochschulen in den Bereichen Ausbildung und Forschung ist ein großes Potenzial für Forschungsberichte vorhanden. In die Berichtreihe werden sowohl hervorragende Diplom- und Projektarbeiten und Dissertationen als auch Forschungsberichte der Institutsmitarbeiter und Institutsgäste zu aktuellen Fragen der Techno- und Wirtschaftsmathematik aufgenommen.

Darüber hinaus bietet die Reihe ein Forum für die Berichterstattung über die zahlreichen Kooperationsprojekte des Instituts mit Partnern aus Industrie und Wirtschaft.

Berichterstattung heißt hier Dokumentation des Transfers aktueller Ergebnisse aus mathematischer Forschungs- und Entwicklungsarbeit in industrielle Anwendungen und Softwareprodukte – und umgekehrt, denn Probleme der Praxis generieren neue interessante mathematische Fragestellungen.

Prof. Dr. Dieter Prätzel-Wolters
Institutsleiter

Kaiserslautern, im Juni 2001

Report on Finite Element Simulations of Electrochemical Processes in Li-ion Batteries with Thermic Effects

M. Taralov [*] , V. Taralova [*], P. Popov[†], O. Iliev [*], A. Latz [*], J. Zausch [*]

[*]Fraunhofer ITWM, Fraunhofer-Platz-1, 67663 Kaiserslautern, Germany

[†]Bulgarian Academy of Sciences, Institute of Information and Communication Technologies, Acad. G. Bonchev St., Block 2, 1113 Sofia, Bulgaria

Acknowledgement

The research was funded in part by Fraunhofer ITWM and EU FP7 project PIRG03-GA-2008-230919 in collaboration with the Bulgarian Academy of Sciences.

Abstract

We present a two dimensional finite element simulation of a thermodynamic electrochemical model of lithium-ion batteries on microscale level. This model consists of several nonlinear equations set in multiple domains. The different domains are coupled with nonlinear interface conditions. Furthermore some of the quantities in the model are discontinuous across these inner boundaries. A node splitting technique is used for the finite element method to account for these discontinuities. The time disretization is done using the backward Euler method. The resulting system of nonlinear equations is solved using Newton's method. Numerical experiments are presented along with physical interpretation of the results.

Contents

List of Tables

List of Figures

List of Symbols

c_e, c_s - concentration of lithium ions in electrolyte and solid particle respectively

Φ_s - electrical potential

φ_e - electrochemical potential

T - temperature

D - interdiffusion coefficient; strictly posivite

t_+ - transference number of Li ions

λ - heat conductivity; strictly positive

κ - electric condictivity; strictly positive

$\mathbf{N}_+$ - ionic flux

$\mathbf{j}$ - electrical current

Π - Peltier coefficient

F - Faraday constant

z_+ - charge of positive ions

R - Universal gas constant

β - Seebek coefficient

k_T - Soret coefficient

c_p - specific heat per unit mass

ρ - mass density

σ - average electronic conductivity

i_0 - amplitude

i_{se} - current density across the interface

η_s - overpotential

μ - chemical potential

U_0 - half cell open circuit potential

$c_{s,max}$ - maximum concentration of ions in the active particle

k - reaction rate

soc - state of charge, i.e. $\frac{c_s}{c_{s,max}}$

1 Introduction

Mathematical modeling of lithium ion batteries is very important. The usage of devices requiring high energy density batteries is increasing every year. Some of the industries using them are mobile phones, computers and cars manufacturers. The highest energy density rechargable batteries are the li-ion batteries. Mathematical models describing their work can be used by battery manufacturers to help choose the right materials to increase even further their capacity. Furthermore, with the right tools, dangerous scenarios could be identified thus ensuring safe working conditions. Also of interest, is not only the time needed to discharge the battery, but also the time needed to charge it. The lifetime of the battery expressed in number of charge/discharge cycles could also be improved. The structure and operation of the batteries described in Section 1.1 and Section 1.2 are based on [13].

1.1 Structure of a li-ion battery

Li-ion batteries are multiscale systems. On the top level we have a battery pack. This battery pack contains one or more cells. We are considering the micro lengthscale where the structure of these cells is resolved. Their main components, and by extension the battery's main components, are anode, cathode, electorlyte and separator. The anode and the cathode are commonly referred to as electrodes. What is common for them is that they have porous structure. Both the anode and the cathode are made of multiple small particles connected together. These particles are on micro or even nano scale. The anode is the negative electrode and the cathode is the positive electrode. The electrolyte is typically non-aqueous liqiud made of a lithium salt dissolved into organic solvent. This is due to the fact that lithium is very reactive with water. The electrodes are made of solid materials in which lithium can enter and exit due to electrochemical reactions. The two are physically separated by the separator so that the battery will not short-circuit. The separator is also with a porous structure. The electrolyte fills the whole empty space between the different components of the cell.

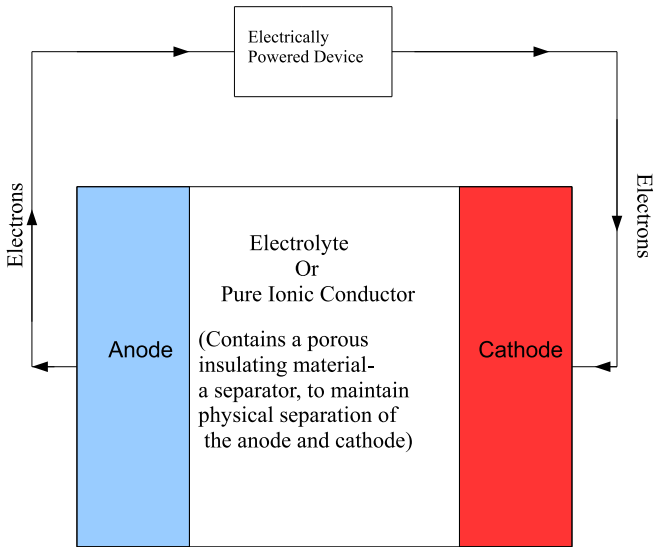

Figure 1: Battery Scheme

1.2 Electrochemical processes in a li-ion battery

The main process inside the battery is the diffusion and migration i.e. potential driven flux of lithium ions. The process of a lithium ion entering in an electrode is called intercalation. The

inverse process of a lithium-ion leaving an electrode is called deintercalation. These electrochemical reactions of intercalation and deintercalation happen on the interface between the electrodes and the electrolyte. During discharge of the battery, i.e. when a power consuming device is connected to the battery, the lithium ions diffuse to the surface of the active particles of the anode, deintercalate into the electrolyte phase and carry then the electric current from the negative to the positive electrode through the pores of the separator. There the ions are intercalated into the active particles and diffuse into the particles. The electrical curent within the active particles is mainly carried by electrons. The electrons do not enter the electrolyte phase. Only the Li-ions can move through the electrolyte. Therefore the particles in the electrodes have to be connected to each other to guarantee the electric conductivity of the electrode as a whole. The electrical current i.e the electrons leave the cell through current collectors, which are connected to the active material. This is shown in Figure 2.

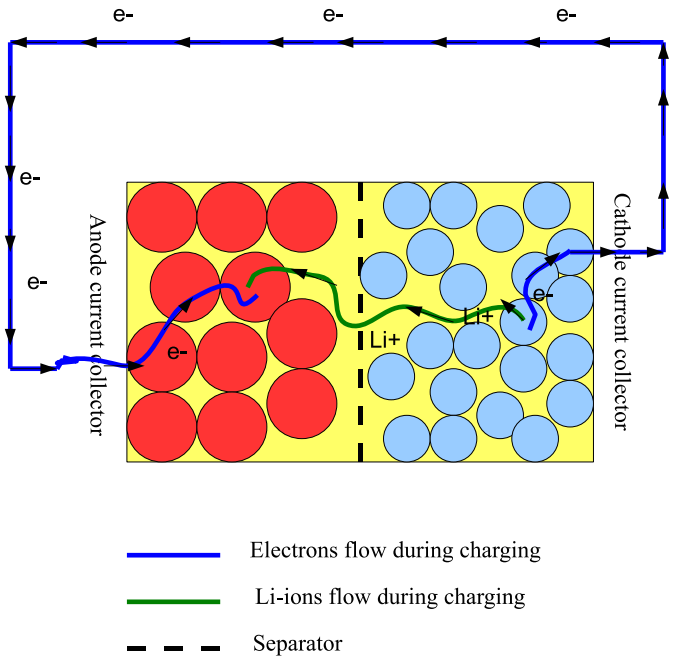

Figure 2: Micro scale charging of a battery cell

When the battery is being charged a higher voltage than the one produced by the battery is applied on the cathode thus forcing the current to pass from the cathode to the anode. During the operation of the battery the temperature may rise significantly. Heat is one of the major contributors to the degradation of the materials inside the battery [23, 2]. It can also lead to unsafe working conditions caused by a local hotspot somewhere inside the cell. As such the full mathematical model described in [10] will be used in this work. Resolving the microscale structure of lithium ion batteries is a crucial part of understanding the physical and electrochemical processes in these batteries. A battery cannot be indefinitely charged and discharged without gradual loss of charge capacity and power capability. The active materials in the electrodes tend to react chemically with the electrolyte. The reaction products form protective surface layers on electrode surfaces, which stop or slow down these chemical surface reactions. After many cycles of charging and discharging, the instability of these surface layers contributes to both power fade and capacity loss in lithium-ion-cell chemistries. Therefore, in order to find ways to slow these degradation processes down, we need to detect and describe these processes and to understand their mechanism and kinetics. Interfacial phenomena takes place at nano- or microscales and can be characterized only by careful investigation of the processes occuring at the interface between

the active particles and the electrolyte. Therefore the main contribution of the model [10] is that it considers separately the complex transport phenomena in the active particles of the electrodes and in the electrolyte on microscale. To the best of our knowledge, there is little literature regarding systematic derivation of thermodynamically consistent microscale Li-ion battery models. A lot of the simulations are based on the pseudo 2D model of Newman et. al. and use finite differences [14]. The early FORTRAN codes are supplied by Newman himself in his BAND routine. This model is widely used since due to its 1D+1D nature it is both easy to implement and also runs very fast. It is not thermodynamic, but there are thermal extensions based on global energy conservasion, i.e. usually without considering the microstructure of the battery and also using a prescribed heat generator [3, 4, 16]. In order to account for the interface conditions more naturally there are also Finite Volume or Finite Element discretizations. If one wants to also observe local phenomena a cell resolved model could be used. They are far more expensive to solve however (especially in 3D) so simulating many charge/discharge cycles can take a lot of time. For an example of finite volume discretization of a cell resolved isothermal model [11], see [17, 12]. A cell-resolved model was solved in [6] with finite elements, using Comsol. With finite elements the coupling conditions can be expressed as natural boundary conditions. This motivates us to use FEM in our simulations.

2 Mathematical model

We consider both [10] and the previously derived [11] models. The first model is thermodynamic and the second one is isothermal. Due to the similarity in the equations, the differences in the models are outlined with a different color. These models are set on the microscale level. The equations describing the mathematical model of the li-ion batteries are different in the electrodes and the electrolyte. In that sense the system of equations will be presented separately in their respective regions. The main processes described in the model are the transport of lithium ions and the transport of charges. It also considers the heat transport and the related variable temperature influence over the ion and charge transport. It is important to account for the variance of the temperature instead of taking an average value over the cell due to the reasons mentioned in Section 1.2. The unkowns in these equations will be the concentration of lithium ions $\left[\frac{mol}{cm^3}\right]$, the electrical (or electrochemical in the electrolyte) potential $[V]$ and the temperature $[K]$. They will be denoted by c, Φ, T respectively. It follows from physical considerations that the functions for the concentration and the potential are discontinuous along the interface. The temperature is continuous there but the heat flux is discontinuous. The set of equations in the system is nonlinear both in the active particles and in the electrolyte. Furthermore since most of the electrochemical reactions are on the interface, the coupling conditions are complex and highly nonlinear. For that reason they will also be presented distinctly from both the equations in the electrolyte and the solids. The full list of the physical symbols, along with short descriptions, is given in the list of symbols on page vii. Since many of these parameters have the same meaning in all regions the lower indices, which indicate whether we are in solid particles or in electrolyte, are omitted in the list. However we note that they have many orders of magnitude difference in the separate regions.

2.1 Equations of the electrolyte

Let us introduce the flux of ion and the flux of charge:

$$\mathbf{N}_{+,e} = -\left(D_e \nabla c_e - \frac{t_+}{z_+ F}\mathbf{j}_e + \frac{D_e c_e k_{T,e}}{T}\nabla T\right) \tag{2.1}$$

$$\mathbf{j}_e = -\left(\kappa \nabla \varphi_e - \kappa \frac{1-t_+}{z_+ F}\left(\frac{\partial \mu_e}{\partial c_e}\right)\nabla c_e - \kappa \frac{1}{z_+ F}\left(\frac{\partial \mu_e}{\partial T}\right)\nabla T\right) \tag{2.2}$$

Then in the electrolyte the system of equations has the following form:

$$\frac{\partial c_e}{\partial t} = -\nabla \cdot \mathbf{N}_{+,e} \tag{2.3a}$$

$$0 = -\nabla \cdot \mathbf{j}_e \tag{2.3b}$$

$$c_{p,e}\rho \frac{\partial T}{\partial t} = \nabla \cdot (\lambda_e \nabla T) + \frac{|\mathbf{j}_e|^2}{\kappa} + \frac{\partial \mu_e}{\partial c_e}\frac{(\mathbf{N}_{+,e} - \frac{t_+}{F z_+}\mathbf{j}_e)^2}{D_e} - T\nabla \cdot \left(c_e \frac{\partial \mu_e}{\partial c_e}\frac{k_{T,e}}{T}\left(\mathbf{N}_{+,e} - \frac{t_+}{F z_+}\mathbf{j}_e\right)\right) \tag{2.3c}$$

These equations describe the li-ion transport, charge transport and heat transport respectively. They are set only in this part of the domain which corresponds to the electrolyte. For the boundary conditions we set zero Neumann for the ionic flux and the electrical current. Physically this means that there is no flow of ions and charge through the boundary of the electrolyte. As no absolute inslulation can be made for the temperature appropriate boundary conditions must be set. We use either Neumann or Robin boundary conditions. We note that in the electrolyte instead of the electrical potential we have the electrochemical potential.

2.2 Equations of the solids

We move on to the system in the electrodes. In the solid particles the ion transference number t_+ is approximately zero, since the current is mainly carried by electrons. In the solids the fluxes are in the following form:

$$\mathbf{N}_{+,s} = -\left(D_s \nabla c_s + \frac{D_s c_s k_{T,s}}{T} \nabla T\right) \tag{2.4}$$

$$\mathbf{j}_s = -\sigma \nabla \Phi_s \tag{2.5}$$

and the equations are:

$$\frac{\partial c_s}{\partial t} = -\nabla \cdot \mathbf{N}_{+,s} \tag{2.6a}$$

$$0 = -\nabla \cdot \mathbf{j}_s \tag{2.6b}$$

$$\begin{aligned} c_{p,s}\rho \frac{\partial T}{\partial t} =& \nabla \cdot (\lambda_s \nabla T) + \frac{|\mathbf{j}_s|^2}{\kappa} - z_+ F \frac{\partial U_0}{\partial c_s} \frac{|\mathbf{N}_{+,s}|^2}{D_s} + \\ & T z_+ F \nabla \cdot \left(c_s \frac{\partial U_0}{\partial c_s} \frac{k_{T,s}}{T} \mathbf{N}_{+,s}\right) \end{aligned} \tag{2.6c}$$

The domain for these equations is either the cathode or the anode. The equations have the same form in both electrodes. The material parameters however are different in the two electrodes. For boundary conditions on the concentration of li-ions we again use zero Neumann on the ionic flux. As was the case for the electrolyte this ensures no flow of ions. This comes naturally because the battery cell is insulated with regard to the li-ions. This means that the amount of ions remains constant throughout the battery. For the potential however the boundary conditions are no longer zero Neumann. We use either non-zero Neumann or Dirichlet boundary conditions. For the temperature we again use either non-zero Neumann or Robin boundary conditions.

2.3 Interface conditions

The interface conditions come from the Butler-Volmer theory. If both a cathodic and an anodic reaction happen in the same electrode the Butler-Volmer equation will give the connection between the electrical current and the potential in the electrode.

$$i_{se} = i_0 \left(\exp\left(\frac{\alpha_a F}{RT}\eta_s\right) - \exp\left(\frac{-\alpha_c F}{RT}\eta_s\right)\right), \tag{2.7}$$

where α_a and α_c are the weights of the anodic and cathodic contributions of the overpotential η_s to the overall reaction. For them we have $\alpha_a + \alpha_c = 1$. For the amplitude i_0 we have

$$i_0 = k c_e^{\alpha_a} c_s^{\alpha_a} (c_{s,max} - c_s)^{\alpha_c} \tag{2.8}$$

The overpotential is expressed in terms of the electrical potential in the electrodes and the electrochemical potential in the electrolyte:

$$\eta_s := \Phi_s - \varphi_e - U_0 \tag{2.9}$$

Finally for the first two equations of the model we have the following interface conditions

$$\mathbf{j}_s \cdot \mathbf{n}_s = \mathbf{j}_e \cdot \mathbf{n}_s = i_{se} = \mathcal{J}(c_e, c_s, \varphi_e, \Phi_s, T) \tag{2.10a}$$

$$\mathbf{N}_{+,s} \cdot \mathbf{n}_s = \mathbf{N}_{+,e} \cdot \mathbf{n}_s = \frac{i_{se}}{z_+ F} = \mathcal{N}(c_e, c_s, \varphi_e, \Phi_s, T) \tag{2.10b}$$

where $\mathbf{n}_s$ is the unit normal vector going out of the solid into the electrolyte. The thermal interface conditions are given by

$$\begin{aligned} -\lambda_s \mathbf{n_s} \cdot \nabla T_s + \lambda_e \mathbf{n_s} \cdot \nabla T_e = \\ - i_{se}\eta_s - i_{se}\Pi + i_{se}\left(c_s \frac{\partial U_0}{\partial c} k_{T,s} + c_e \frac{\partial \mu_e}{\partial c} \frac{k_{T,e}(1-t_+)}{z_+ F} \right) \end{aligned} \tag{2.11}$$

with Π being the Peltier coefficient:

$$\Pi = T(\beta_s - \beta_e) + T \frac{\partial (U_0 + \frac{\mu_e}{z_+ F})}{\partial T}$$

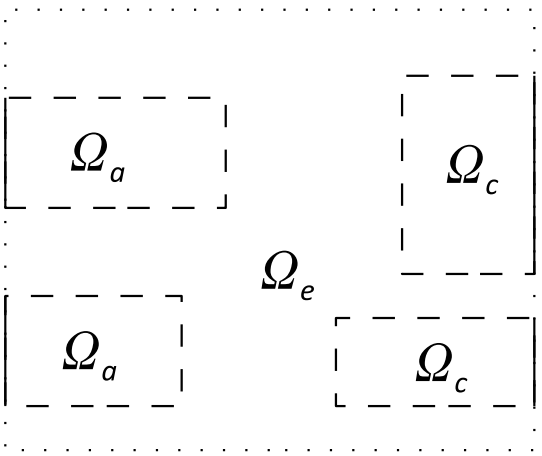

Figure 4: Boundaries for the sample domain shown in Figure 3. The boundaries for the active particles are the solid lines, the ones for the electrolyte are the dotted lines and the interface is given in dashed lines.

3 Weak formulation

In this section we derive the weak formulation for the model presented in Section 2. First we present the functional spaces which we use. Then the weak formulation for each of the regions is derived in their respective sections. The interface conditions are included separately. We denote the domain of the whole cell by Ω. In Ω we further distinguish between three subdomains. The subdomain for the anode is denoted by Ω_a. The one for the cathode is denoted by Ω_c. Finally the one for the electrolyte is denoted by Ω_e. Ω_a and Ω_c themselves can be the union of multiple subdomains. This represents electrodes with multiple particles. A sample domain is shown in Figure 3.

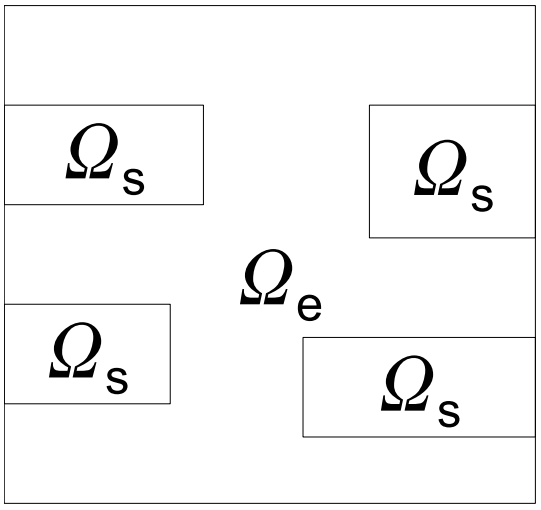

Figure 3: Sample domain for a battery. The whole domain is Ω. The domains for the anode Ω_a and the cathode Ω_c consist of multiple subdomains. The domain of the electrolyte is $\Omega_e = \Omega \backslash (\Omega_a \cup \Omega_c)$.

The boundaries of each domain are shown in Figure 4. Speciffically we have $\partial\Omega_{e,outer} = \partial\Omega \cap \partial\Omega_e$, $\partial\Omega_{a,outer} = \partial\Omega \cap \partial\Omega_a$, $\partial\Omega_{c,outer} = \partial\Omega \cap \partial\Omega_c$ for the outer boundaries of each subdomain and $\Gamma = \partial\Omega_e \backslash \partial\Omega_{e,outer}$ for the interface. The inner interface boundaries are the same for the electrolyte and the solid particles.

3.1 Functional spaces

We use the standart $L^2(\Omega)$ and $H^1(\Omega)$ spaces [19, 7]. Let us remind that L^2 is the space of square integrable functions in Ω

$$L^2(\Omega) = \left\{ v(\mathbf{x}), \mathbf{x} \in \Omega : \int\limits_{\Omega} |v|^2 \, \mathrm{d}\mathbf{x} < \infty \right\}$$

along with the norm:

$$||u||_{L^2(\Omega)} = \left(\int\limits_{\Omega} |u|^2 \, \mathrm{d}\mathbf{x} \right)^{\frac{1}{2}}$$

and $H^1(\Omega)$ is the space whose elements and their derivatives are square integrable, i.e.

$$H^1(\Omega) = \{ v(\mathbf{x}), \mathbf{x} \in \Omega : v \in L^2(\Omega), (\nabla v) \in (L^2(\Omega))^n \}$$

with the norm

$$||u||_{H^1(\Omega)} = \left(\int\limits_{\Omega} u^2 \mathrm{d}\mathbf{x} + \sum_{k=1}^{n} \int\limits_{\Omega} \left(\frac{\partial u}{\partial x_k} \right)^2 \mathrm{d}\mathbf{x} \right)^{\frac{1}{2}}.$$

It is obvious from the definition of L^2 that the functions in this space can be discontinuous. Also functions, which vary only on a subspace of Ω with a Lesbegue measure zero, are equivalent in $L^2(\Omega)$.
We use the standart vector calculus notation, i.e. $\nabla = \left(\frac{\partial}{\partial x_1}, \ldots, \frac{\partial}{\partial x_n} \right)$

3.2 Weak formulation in the electrolyte

In this section we will derive the weak formulation of the electrolyte model equations. Let us recall Equation 2.3a:

$$\frac{\partial c_e}{\partial t} = \nabla \cdot (D_e \nabla c_e) - \nabla \cdot \left(\frac{t_+}{z_+ F} \mathbf{j}_e \right) + \nabla \cdot \left(\frac{D_e c_e k_{T,e}}{T} \nabla T \right)$$

We multiply this equation with a test function $v \in V_1$ where the test space $V_1 = H^1(\Omega)$. After that we integrate over Ω_e to obtain:

$$\int_{\Omega_e} \frac{\partial c_e}{\partial t} v d\mathbf{x} = \int_{\Omega_e} \nabla \cdot \left(D_e \nabla c_e - \frac{t_+}{z_+ F} \mathbf{j}_e + \frac{D_e c_e k_{T,e}}{T} \nabla T \right) v d\mathbf{x} \tag{3.1}$$

Now we use integration by parts

$$\begin{aligned} \int\limits_{\Omega_e} \frac{\partial c_e}{\partial t} v d\mathbf{x} &= \int\limits_{\Omega_e} \nabla \cdot \left(D_e \nabla c_e - \frac{t_+}{z_+ F} \mathbf{j}_e + \frac{D_e c_e k_{T,e}}{T} \nabla T \right) v d\mathbf{x} \\ &= \int\limits_{\partial \Omega_e} \left[v \left(D_e \nabla c_e - \frac{t_+}{z_+ F} \mathbf{j}_e + \frac{D_e c_e k_{T,e}}{T} \nabla T \right) \right] \cdot \mathbf{n}_e d\mathbf{x} - \\ &\quad \int\limits_{\Omega_e} \left(D_e \nabla c_e - \frac{t_+}{z_+ F} \mathbf{j}_e + \frac{D_e c_e k_{T,e}}{T} \nabla T \right) \cdot \nabla v d\mathbf{x} \end{aligned} \tag{3.2}$$

Thus we obtain the weak formulation of Equation 2.3a. Since the differential equation is nonlinear, analytical estimates of the regularity of the unknown functions are not trivial to obtain. Therefore

we will assume that they are regular enough to be at least $H^1(\Omega)$. We will recall that we have zero Neumann boundary conditions for the electrical current and the ionic flux on the outer boundary of the electrolyte, i.e.

$$\mathbf{N}_+ \cdot \mathbf{n} = 0 \text{ on } \partial\Omega \cap \partial\Omega_e \tag{3.3}$$
$$\mathbf{j} \cdot \mathbf{n} = 0 \text{ on } \partial\Omega \cap \partial\Omega_e \tag{3.4}$$

and we impose Robin boundary conditions for the temperature, i.e.

$$\lambda \frac{\partial T}{\partial \mathbf{n}} = g(T) \text{ on } \partial\Omega \cap \partial\Omega_e \tag{3.5}$$

With these considerations in mind let us look at the boundary integral

$$\int\limits_{\partial\Omega_e} \left[v \left(D_e \nabla c_e - \frac{t_+}{z_+ F} \mathbf{j}_e + \frac{D_e c_e k_{T,e}}{T} \nabla T \right) \right] \cdot \mathbf{n}_e \mathrm{d}s = \int\limits_{\partial\Omega_e} v \mathbf{N}_+ \cdot \mathbf{n}_e \mathrm{d}s = 0 \tag{3.6}$$

The interface conditions will be included separately.
For the weak formulation of Equation 2.3b we have:

$$0 = \int\limits_{\Omega_e} \nabla v (\kappa \nabla \varphi_e) \mathrm{d}\mathbf{x} - \int\limits_{\Omega_e} \nabla v \left(\kappa \frac{1 - t_+}{z_+ F} \left(\frac{\partial \mu_e}{\partial c_e} \right) \nabla c_e \right) \mathrm{d}\mathbf{x} - \int\limits_{\Omega_e} \nabla v \left(\kappa \frac{1}{z_+ F} \left(\frac{\partial \mu_e}{\partial T} \right) \nabla T \right) \mathrm{d}\mathbf{x} \tag{3.7}$$

For Equation 2.3c we again multiply by a test function and integrate over Ω_e

$$\begin{aligned}
\int\limits_{\Omega_e} v c_{p,e} \rho \frac{\partial T}{\partial t} \mathrm{d}\mathbf{x} = & \int\limits_{\Omega_e} v \nabla \cdot (\lambda_e \nabla T) \mathrm{d}\mathbf{x} + \int\limits_{\Omega_e} v \frac{|\mathbf{j}_e|^2}{\kappa} \mathrm{d}\mathbf{x} + \int\limits_{\Omega_e} v \frac{\partial \mu_e}{\partial c_e} \frac{(\mathbf{N}_{+,e} - \frac{t_+}{F z_+} \mathbf{j}_e)^2}{D_e} \mathrm{d}\mathbf{x} - \\
& \int\limits_{\Omega_e} v T \nabla \cdot \left(c_e \frac{\partial \mu_e}{\partial c_e} \frac{k_{T,e}}{T} \left(\mathbf{N}_{+,e} - \frac{t_+}{F z_+} \mathbf{j}_e \right) \right) \mathrm{d}\mathbf{x} \\
= & - \int\limits_{\Omega_e} \nabla v \cdot (\lambda_e \nabla T) \mathrm{d}\mathbf{x} + \int\limits_{\Omega_e} v \frac{|\mathbf{j}_e|^2}{\kappa} \mathrm{d}\mathbf{x} + \int\limits_{\Omega_e} v \frac{\partial \mu_e}{\partial c_e} \frac{(\mathbf{N}_{+,e} - \frac{t_+}{F z_+} \mathbf{j}_e)^2}{D_e} \mathrm{d}\mathbf{x} + \\
& \int\limits_{\Omega_e} \nabla (v T) \cdot \left(c_e \frac{\partial \mu_e}{\partial c_e} \frac{k_{T,e}}{T} \left(\mathbf{N}_{+,e} - \frac{t_+}{F z_+} \mathbf{j}_e \right) \right) \mathrm{d}\mathbf{x} + \\
& \int\limits_{\partial\Omega_e} v \lambda_e \nabla T \cdot \mathbf{n}_e \mathrm{d}s - \int\limits_{\partial\Omega_e} v T \left(c_e \frac{\partial \mu_e}{\partial c_e} \frac{k_{T,e}}{T} \left(\mathbf{N}_{+,e} - \frac{t_+}{F z_+} \mathbf{j}_e \right) \right) \cdot \mathbf{n}_e \mathrm{d}s
\end{aligned} \tag{3.8}$$

where we also used integration by parts.
The equations of the electrolyte then have the following form

$$\int\limits_{\Omega_e} \frac{\partial c_e}{\partial t} v \mathrm{d}\mathbf{x} - \int\limits_{\Omega_e} \left(D_e \nabla c_e - \frac{t_+}{F} \mathbf{j}_e + \frac{D_e c_e k_{T,e}}{T} \nabla T \right) \cdot \nabla v d\mathbf{x} = 0 \tag{3.9a}$$

$$\int\limits_{\Omega_e} (\kappa \nabla \varphi_e) \cdot \nabla v \mathrm{d}\mathbf{x} - \int\limits_{\Omega_e} \left(\kappa \frac{(1 - t_+) RT}{F c_e} \nabla c_e \right) \cdot \nabla v \mathrm{d}\mathbf{x} - \int\limits_{\Omega_e} \left(\kappa \frac{R \ln c_e}{F} \nabla T \right) \cdot \nabla v \mathrm{d}\mathbf{x} = 0 \tag{3.9b}$$

$$\begin{aligned}
& \int\limits_{\Omega_e} v c_{p,e} \rho \frac{\partial T}{\partial t} \mathrm{d}\mathbf{x} = - \int\limits_{\Omega_e} \nabla v \cdot (\lambda_e \nabla T) \mathrm{d}\mathbf{x} + \int\limits_{\Omega_e} v \frac{|\mathbf{j}_e|^2}{\kappa} \mathrm{d}\mathbf{x} + \int\limits_{\Omega_e} v \frac{\partial \mu_e}{\partial c_e} \frac{(\mathbf{N}_{+,e} - \frac{t_+}{F} \mathbf{j}_e)^2}{D_e} \mathrm{d}\mathbf{x} + \\
& \int\limits_{\Omega_e} \nabla (v T) \cdot \left(R k_{T,e} \left(\mathbf{N}_{+,e} - \frac{t_+}{F} \mathbf{j}_e \right) \right) \mathrm{d}\mathbf{x} + \int\limits_{\partial\Omega_{e,outer}} v g(T) \mathrm{d}s
\end{aligned} \tag{3.9c}$$

As noted before the interface conditions will be accounted for separately. This means that all boundary integrals in this section are to be understood over $\partial\Omega_{e,outer}$ and the interface integrals are omitted.
We will also mention that the spaces of the test function for the second and third equations, i.e. V_2 and V_3 are also $H^1(\Omega_e)$.

3.3 Weak formulation in the active particles

The weak formulation in the active particles is obtained in the same manner as the one for the electrolyte so we will not do it thoroughly. We will note however the difference in the boundary conditions for the potential. Since the equations have the exact same form in the two types of active particles we will use $\Omega_s = \Omega_a \cup \Omega_c$ along with $\partial\Omega_{s,outer} = \partial\Omega_{a,outer} \cup \partial\Omega_{c,outer}$. The weak formulation for Equation 2.6a,Equation 2.6b and Equation 2.6c is

$$\int_{\Omega_s} \frac{\partial c_s}{\partial t} v \mathrm{d}\mathbf{x} + \int_{\Omega_s} (D_s \nabla c_s) \cdot \nabla v \mathrm{d}\mathbf{x} + \int_{\Omega_s} \left(\frac{D_s c_s k_{T,s}}{T} \nabla T \right) \cdot \nabla v \mathrm{d}\mathbf{x} = 0 \tag{3.10a}$$

$$\int_{\Omega_s} (\sigma \nabla \Phi_s) \cdot \nabla v \mathrm{d}\mathbf{x} - \int_{\partial\Omega_{s,outer}} i_{appl} v \mathrm{d}s = 0 \tag{3.10b}$$

$$\int_{\Omega_s} v c_{p,s} \rho \frac{\partial T}{\partial t} \mathrm{d}\mathbf{x} = -\int_{\Omega_s} \nabla v \cdot (\lambda_s \nabla T) \mathrm{d}\mathbf{x} + \int_{\partial\Omega_{s,outer}} v g(T) \mathrm{d}s + \int_{\Omega_s} v \frac{|\mathbf{j}_s|^2}{\kappa} \mathrm{d}\mathbf{x} - \int_{\Omega_s} v F \frac{\partial U_0}{\partial c_s} \frac{|\mathbf{N}_{+,s}|^2}{D_s} \mathrm{d}\mathbf{x} - \int_{\Omega_s} \nabla(vT) \cdot \left(c_s F \frac{\partial U_0}{\partial c_s} \frac{k_{T,s}}{T} \mathbf{N}_{+,s} \right) \mathrm{d}\mathbf{x} \tag{3.10c}$$

The boundary integral in Equation 3.10b comes from the non-zero Neumann conditions. The test spaces in the solid particles are

$$V_{1,s}(\Omega_s) = V_{2,s}(\Omega_s) = V_{3,s}(\Omega_s) = H^1(\Omega_s)$$

where $V_{1,s}(\Omega_s), V_{2,s}(\Omega_s), V_{3,s}(\Omega_s)$ are the test spaces for the test function in Equation 3.10a, Equation 3.10b and Equation 3.10c respectively. Again we omit here the integral over Γ which will be added in Section 3.4.

3.4 The whole domain and the interface conditions

Let us now consider what happens on the whole domain Ω. Globally our test spaces for the first two equations can be discontinuous across the interface. So we have $V_1(\Omega) = V_2(\Omega) = L^2(\Omega)$. Also for the first two equations it is trivial to account for the interface conditions by simply adding the interface integrals in their respective weak formulations in both regions. This means that we subtract from the left hand side of Equation 3.9a and add to the left hand side of Equation 3.10a the following term

$$\int_{\Gamma} \mathcal{N} v \mathrm{d}s$$

We subtracted from Equation 3.9a because our interface conditions are given in terms of the normal from the particle so we must take $\mathbf{n}_e = -\mathbf{n}_s$. Analogously we subtract from Equation 3.9b and add to Equation 3.10b

$$\int_{\Gamma} \mathcal{J} v \mathrm{d}s$$

Although the equations can be summed and given in a single domain in the terms of discontinuous coefficients it is more convinient for us for them to be in this form.

For the heat transport equation however we have to sum the equations in a single domain to obtain the interface integrals neccessary for the weak formulation. Furthermore since the temperature is continuous across the interface we can require of our test space $V_3(\Omega)$ to be $H^1(\Omega)$. This means that we can consider the test functions to be continuous and so have the same value on both sides of the interface. Since the equations are long and the integrals over the subdomains and the outer boundaries do not change we restrict our calculations to the interface integrals.

$$\begin{aligned}
&\int_\Gamma v\lambda_e \nabla T_e \cdot \mathbf{n}_e \mathrm{d}s + \int_\Gamma v\lambda_s \nabla T_s \cdot \mathbf{n}_s \mathrm{d}s - \\
&\int_\Gamma vT\left(c_e \frac{\partial \mu_e}{\partial c_e}\frac{k_{T,e}}{T}\left(\mathbf{N}_{+,e} - \frac{t_+}{F}\mathbf{j}_e\right)\right)\cdot \mathbf{n}_e \mathrm{d}s + \\
&\int_\Gamma vT\left(c_s F \frac{\partial U_0}{\partial c_s}\frac{k_{T,s}}{T}\mathbf{N}_{+,s}\right)\cdot \mathbf{n}_s \mathrm{d}s
\end{aligned} \tag{3.11}$$

after we use Equation 2.10a,Equation 2.10b and Equation 2.11 we get

$$\begin{aligned}
&-\int_\Gamma v\left[-i_{se}\eta_s - i_{se}\Pi + i_{se}\left(c_s\frac{\partial U_0}{\partial c}k_{T,s} + c_e\frac{\partial \mu_e}{\partial c}\frac{k_{T,e}(1-t_+)}{z_+F}\right)\right]\mathrm{d}s + \\
&\int_\Gamma v\left(c_e\frac{\partial \mu_e}{\partial c_e}k_{T,e}\left(\mathcal{N} - \frac{t_+}{F}\mathcal{J}\right)\right)\mathrm{d}s + \int_\Gamma v\left(c_s F\frac{\partial U_0}{\partial c_s}k_{T,s}\mathcal{N}\right)\mathrm{d}s = \\
&\int_\Gamma v i_{se}(\eta_s + \Pi)\mathrm{d}s = \int_\Gamma v\mathcal{T}\mathrm{d}s
\end{aligned} \tag{3.12}$$

Therefore the heat transport equation becomes

$$\begin{aligned}
&\int_\Omega vc_p\rho\frac{\partial T}{\partial t}\mathrm{d}\mathbf{x} = -\int_\Omega \nabla v\cdot(\lambda\nabla T)\mathrm{d}\mathbf{x} + \int_\Omega v\frac{|\mathbf{j}|^2}{\kappa}\mathrm{d}\mathbf{x} + \int_\Omega v\frac{\partial\mu}{\partial c}\frac{(\mathbf{N}_+ - \frac{t_+}{F}\mathbf{j})^2}{D}\mathrm{d}\mathbf{x} + \\
&\int_\Omega \nabla(vT)\cdot\left(c\frac{\partial\mu}{\partial c}\frac{k_T}{T}(\mathbf{N}_+ - \frac{t_+}{F}\mathbf{j})\right)\mathrm{d}\mathbf{x} + \int_{\partial\Omega} v\lambda g(T)\mathrm{d}s - \\
&\int_{\partial\Omega} vT\left(c\frac{\partial\mu}{\partial c}\frac{k_T}{T}(\mathbf{N}_+ - \frac{t_+}{F}\mathbf{j})\right)\cdot\mathbf{n}\mathrm{d}s + \int_\Gamma v\mathcal{T}\mathrm{d}s
\end{aligned} \tag{3.13}$$

where t_+ is nonzero only in the electrolyte and

$$\mu = \begin{cases} \mu_0 + RT\ln c, & \mathbf{x}\in\Omega_e \\ \mu_{Li} - FU_0, & \mathbf{x}\in\Omega_s \end{cases} \tag{3.14}$$

Remark. Notice that we have not accounted for the Dirichlet boundary conditions. Generally it is not so trivial to apply them to a function in $H^1(\Omega)$ since they have no meaning on a set of measure zero like the boundary has with regards to measure of Ω. For a rigorous analysis we must also introduce the notion of traces. However to avoid further complicating the functional analysis part we will assume that the unknown function is continuous on the boundary and we can take its restriction there. For further information, c.f. [19, 7].

Remark. The spaces which we discussed are considered only for the variables in space. We assume that the unknown functions are continuously differentiable in time.

4 Numerical methods

We use several different methods in order to solve our system of equations. First we need to discretize the problem in the spatial variables. We use the Finite Element method [1, 5, 18]. After that for the time discretization we use the Backward Euler method [8]. Since this method is implicit it results in a system of nonlinear equations. We linearize this system with the Newton method [15, 9]. Finally for the linear system we use the ILUT preconditioned BiCGSTAB method [22] or the commercial library SAMG. The latter is not discussed here but it is an implementation of algebraic multigrid. They are implemented in code using the C++ programming language. Double precision is used for all floating point variables.

4.1 Finite Element Method

Let us consider the equations we derived in the weak formulation in Section 3. Instead of the full spaces $V_i(\Omega)$ however we take finite dimensional subspaces of them $V_{i,h} \subset V_i$. We also take the unknown functions to be in these spaces, i.e. $c, \Phi, \varphi, T \in V_{3,h}(\Omega)$. We denote these restrictions of the functions by $c_h, \Phi_h, \varphi_h, T_h$. Without making any further modifications to the weak formulations we have our discrete problem. Such an approximation is known as Ritz-Galerkin approximation. Now we look for a suitable basis for this space. We describe this process in two dimensions. First we divide the domain Ω into triangles as shown in Figure 5.

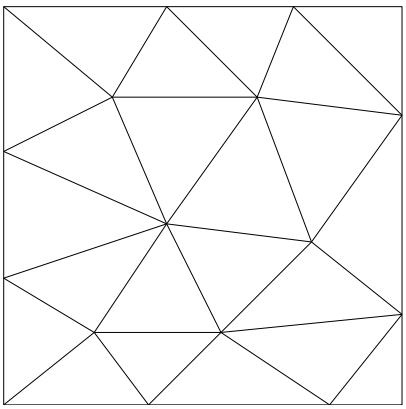

Figure 5: Triangulation of a region

This process is known as triangulation. We can use other shapes but we restrict ourselves to triangles. We denote these triangles by e_i and call them elements, and their vertices are denoted by p_i. Let us now consider the polynomials of certain order over these elements, i.e.

$$v(\mathbf{x}) : v \in P_k(e_i)$$

Along with these polynomials let us consider a set of functionals over the elements acting upon them. The simplest possible combination would be polynomials of first order together with the functionals which take the value of a function at the vertices of the triangles. Then for the basis of a finite dimensional space we take piecewise polynomials (they are linear polinomials in each triangle) such that the basis function φ_i (not to be confused with the electrochemical potential) is unity only at node p_i and zero at every other node, i.e. $\varphi_i(p_j) = \delta_{ij}$ as depicted in Figure 6a. It follows that the support of these functions, depicted in Figure 6b is limited only to the few elements which contain their associated node.

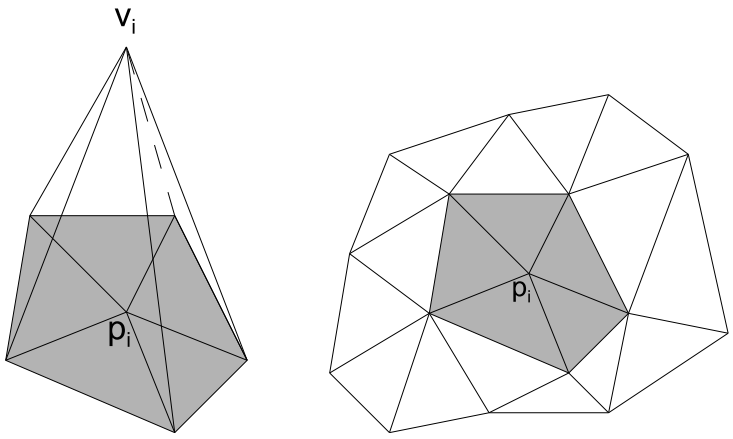

(a) Lagrange basis function at node i

(b) Support of a lagrange basis function

Figure 6: Lagrange basis function at node i

It is easy to check that such basis functions are continuous over the whole domain. Such a basis is called nodal basis and the associated finite elements - Lagrange finite elements. Let us now assume that our functions are regular enough as to be able to get pointwise values at the nodes. Then we call the interpolant of the concentration [1]

$$c_I = \sum_{i=1}^{n} c(p_i)\varphi_i$$

and we have analogous interpolants for the potential and the temperature. To account for the discontinuous concentration and potential we split the nodes on the interface so that the nodes on one side are strictly for the functions in the electrolyte and on the other side - for the solid particle. For reference see Figure 7.

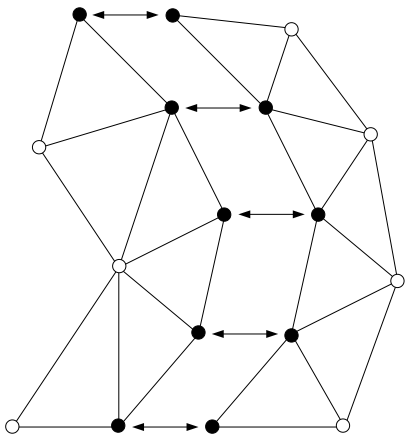

Figure 7: Example of splitting of the nodes on the interface. The split nodes are in black and the others are in white.

Since we formally have different nodes, and hence different basis functions on both sides of the interface, the test functions there are discontinuous, c.f. Figure 8.

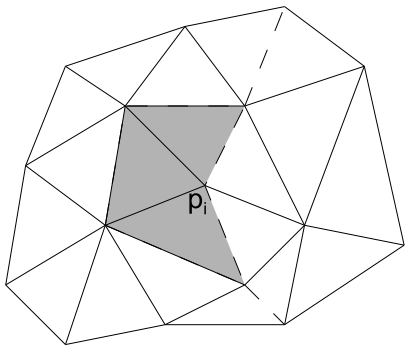

Figure 8: Support of a basis function on a split node. The interface is the dashed line.

Note that this splitting is for V_1 and V_2 whereas the basis functions in V_3 remain continuous even on the interface. Our unknowns in the discretized problem become the nodal values of the unknown functions at each time step. We use the following discretization on the finite basis

$$c_h = \sum_{i=1}^{n_1} C_i(t)\varphi_{1,i}(\mathbf{x})$$
$$P_h = \sum_{i=1}^{n_2} P_i(t)\varphi_{2,i}(\mathbf{x})$$
$$T_h = \sum_{i=1}^{n_3} T_i(t)\varphi_{3,i}(\mathbf{x})$$

where n_1, n_2, n_3 are the dimensions of the finite dimensional test spaces $V_{1,h}(\Omega), V_{2,h}(\Omega)$, $V_{3,h}(\Omega)$, respectively. We note that we have combined potential in the electrodes and the electrochemical potential in the electrolyte in a single function, i.e. $P_h = \varphi_h, \mathbf{x} \in \Omega_e$ and $P_h = \Phi_h, \mathbf{x} \in \Omega_s$. Also note that in this discretization the variables in space are present only in the basis functions while the time variables are only in the unknowns. The theoretical error estimate in the spatial variables for linear elliptic PDEs is of order $O(h^2)$ in the $L^2(\Omega)$ norm where h is the diameter of the triangulation, i.e. the longest edge of a triangle. Let us now show the problem in the electrolyte in discretized form:

$$\int_{\Omega_e} \frac{\partial c_h}{\partial t}\varphi_{1,j}\mathrm{d}\mathbf{x} + \int_{\Omega_e} \left(D_e\nabla c_h - \frac{t_+}{F}\mathbf{j}_e + \frac{D_e c_h k_{T,e}}{T_h}\nabla T_h\right)\cdot\nabla\varphi_{1,j}d\mathbf{x} - \int_{\Gamma}\mathcal{N}\varphi_{1,j}\mathrm{d}s = 0, \quad j = 1,\ldots,\mathrm{n}_1 \tag{4.1a}$$

$$\int_{\Omega_e}(\kappa\nabla P_h)\cdot\nabla\varphi_{2,j}\mathrm{d}\mathbf{x} - \int_{\Omega_e}\left(\kappa\frac{(1-t_+)RT_h}{Fc_h}\nabla c_h\right)\cdot\nabla\varphi_{2,j}\mathrm{d}\mathbf{x} - \int_{\Omega_e}\left(\kappa\frac{R\ln c_h}{F}\nabla T_h\right)\cdot\nabla\varphi_{2,j}\mathrm{d}\mathbf{x} -$$
$$\int_{\Gamma}\mathcal{J}\varphi_{2,j}\mathrm{d}s = 0, \quad j = 1,\ldots,\mathrm{n}_2 \tag{4.1b}$$

$$\int_{\Omega}\varphi_{3,j}c_p\rho\frac{\partial T_h}{\partial t}\mathrm{d}\mathbf{x} + \int_{\Omega}\nabla\varphi_{3,j}\cdot(\lambda\nabla T_h)\mathrm{d}\mathbf{x} - \int_{\Omega}\varphi_{3,j}\frac{|\mathbf{j}|^2}{\kappa}\mathrm{d}\mathbf{x} - \int_{\Omega}\varphi_{3,j}\frac{\partial\mu}{\partial c}\frac{(\mathbf{N}_+ - \frac{t_+}{F}\mathbf{j})^2}{D}\mathrm{d}\mathbf{x} -$$
$$\int_{\Omega}\nabla(\varphi_{3,j}T_h)\cdot\left(c_h\frac{\partial\mu}{\partial c}\frac{k_T}{T_h}\left(\mathbf{N}_+ - \frac{t_+}{F}\mathbf{j}\right)\right)\mathrm{d}\mathbf{x} - \int_{\partial\Omega}\varphi_{3,j}\lambda g(T_h)\mathrm{d}s - \int_{\Gamma}\varphi_{3,j}\mathcal{T}\mathrm{d}s = 0, \quad j = 1,\ldots,\mathrm{n}_3 \tag{4.1c}$$

Due to the small compact support of the basis functions it is obvious that the above integrals are zero over most of the domain. Actually we will be making all of the calculations on a per element basis. This means that intergrals should be considered as

$$\int_{\Omega} = \sum_{k=1}^{number\_of\_elements} \int_{e_k} = \sum_{k:e_k \subset supp(\varphi_i) \cap supp(\varphi_j)} \int_{e_k}$$

However for notational simplicity we will leave them as they are.

4.2 Backward Euler Method

The backward Euler method is of the class of backward differentiation formulas. It can be derived easily. Let us consider the following equation:

$$\frac{\partial u}{\partial t} = f(t, u)$$

If we integtrate on both sides over the interval $[t, t+\tau]$ we get

$$\int_t^{t+\tau} \frac{\partial u}{\partial t} \mathrm{d}t = \int_t^{t+\tau} f(t)\mathrm{d}t \approx \tau f(t+\tau, u(t+\tau))$$
$$\Leftrightarrow u(t+\tau) - u(t) \approx \tau f(t+\tau, u(t+\tau))$$

where for the approximation of the right hand side we have used the formula of the "right" rectangles. The backward Euler method has a first order of accuracy $O(\tau)$. We will note that while it is easy to implement the second order Crank-Nicholson method it can be numerically unstable for nonlinear problems [5]. The backward Euler method is also A-stable as defined by Dahlquist [8]. This method is implicit, i.e. the values for the current time step are used in the right hand side of the equation. This means that in order to obtain the current time step approximation of the unknown function we must solve a system of equations. We will use the following notation

$$C_j(t_l) = C_j^l \tag{4.2}$$
$$c_h(t_l) = c_h^l \tag{4.3}$$

For example when applied to Equation 4.1a the backward Euler method yields:

$$\int_{\Omega_e} \frac{c_h^l - c_h^{l-1}}{\tau} \varphi_{1,j} \mathrm{d}\mathbf{x} + \int_{\Omega_e} \left(D_e \nabla c_h^l - \frac{t_+}{F} \mathbf{j}_e + \frac{D_e c_h^l k_{T,e}}{T_h^l} \nabla T_h^l \right) \cdot \nabla \varphi_{1,j} d\mathbf{x} - \int_{\Gamma} \mathcal{N} \varphi_{1,j} \mathrm{d}s = 0 \tag{4.4}$$

Remark. We could use the explicit forward Euler scheme but for nonlinear problems the time step may become too small for practical use.

4.3 Newton method

One of the drawbacks of the backward Euler method in our case is that the method results in a system of non-linear equations. We will linearize this system with the help of the Newton method. It is a fastly convergent iterative method for solving nonlinear problems. Specifically it has a quadratic order of convergence which means that the error reduces with a quadratic speed at each iteration of the method. Let us denote by $\mathbf{F}_1(\mathbf{C}, \mathbf{P}, \mathbf{T})$ the set of functions on the left hand side of the equations obtained from discretizing the ion transport equation from all the domains. The

unknowns are written as vectors, i.e. $\mathbf{C} = (C_1, \ldots, C_{n_1})$, $\mathbf{P} = (P_1, \ldots, P_{n_2})$, $\mathbf{T} = (T_1, \ldots, T_{n_3})$. Then these equations can be written as

$$\mathbf{F}_1(\mathbf{C}, \mathbf{P}, \mathbf{T}) = 0 \tag{4.5}$$

Analogously we do the same for the charge transport equations with $\mathbf{F}_2(\mathbf{C}, \mathbf{P}, \mathbf{T})$ and the heat transport equations with $\mathbf{F}_3(\mathbf{C}, \mathbf{P}, \mathbf{T})$. Let us also denote $\mathbf{F} = (\mathbf{F}_1, \mathbf{F}_2, \mathbf{F}_3)$. Then for the whole system of equations we have

$$\mathbf{F}(\mathbf{C}, \mathbf{P}, \mathbf{T}) = 0 \tag{4.6}$$

The vector function $\mathbf{F}$ is known as the residual. For the derivation of the method, c.f. [15]. We denote $\mathbf{U} = (\mathbf{C}, \mathbf{P}, \mathbf{T})$ The algorithm itself for Equation 4.6 is as follows:

- pick an initial iterate $\mathbf{U}^{(0)}$
- iterate for $\mathbf{U}^{(k)} = \mathbf{U}^{(k-1)} + \mathbf{d}^k$ until $||\mathbf{F}(\mathbf{U}^{(k)})|| \leq \varepsilon_r ||\mathbf{F}(\mathbf{U}^{(0)})|| + \varepsilon_a$, c.f. [9]

with the search direction $\mathbf{d}^k$ being the solution of the system

$$\mathbf{J}(\mathbf{U}^{k-1})\mathbf{d}^k = -\mathbf{F}(\mathbf{U}^{k-1}) \tag{4.7}$$

where $\mathbf{J}$ is the Jacobian matrix of the vector function $\mathbf{F}$, i.e.

$$\mathbf{J} = \begin{pmatrix} \dfrac{\partial \mathbf{F}_1}{\partial \mathbf{C}} & \dfrac{\partial \mathbf{F}_1}{\partial \mathbf{P}} & \dfrac{\partial \mathbf{F}_1}{\partial \mathbf{T}} \\ \dfrac{\partial \mathbf{F}_2}{\partial \mathbf{C}} & \dfrac{\partial \mathbf{F}_2}{\partial \mathbf{P}} & \dfrac{\partial \mathbf{F}_2}{\partial \mathbf{T}} \\ \dfrac{\partial \mathbf{F}_3}{\partial \mathbf{C}} & \dfrac{\partial \mathbf{F}_3}{\partial \mathbf{P}} & \dfrac{\partial \mathbf{F}_3}{\partial \mathbf{T}} \end{pmatrix} \tag{4.8}$$

Also ε_r is the tolerance of the method for the relative residual, which is $||\mathbf{F}(\mathbf{U}^{(k)})||/||\mathbf{F}(\mathbf{U}^{(0)})||$. ε_a is the tolerance for the absolute residual, which is $||\mathbf{F}(\mathbf{U}^{(k)})||$. It is necessary to test for both since with a good initial iterate we might not be able to achieve the desired tolerance for the relative residual. In our experiments we use $\varepsilon_r = \varepsilon_a = 10^{-6}$. In order for the method to have its quadratic convergence rate, the initial guess must be close to the solution, the Jacobian matrix must be invertible, i.e. nonsingular and the second derivatives of the functions must be bounded. Since the original problem is parabolic we use the solution from the previous time step as an initial guess.

Let us now calculate one of the derivatives for demonstration. The others are done in a similar fashion and some of them will be calculated in Appendix A. We will use the following notation

$$\frac{\partial \mathbf{g}}{\partial y} = \left(\frac{\partial g_1}{\partial y}, \ldots, \frac{\partial g_n}{\partial y} \right)$$

where $\mathbf{g} = (g_1, \ldots, g_n)$ is a vector function and y a scalar variable. We pick for our demonstrative equation the i-th equation of F_1 differentiated with respect to C_j^l. We obtain:

$$\frac{\partial \mathbf{F}_{1,i}}{\partial C_j^l} = \int_{\Omega_e} \frac{\varphi_{1,j}}{\tau} \varphi_{1,i} \mathrm{d}\mathbf{x} + \int_{\Omega_e} \left(D_e \nabla \varphi_{1,j} - \frac{t_+}{F} \frac{\partial \mathbf{j}_e}{\partial c_e} + \frac{D_e \varphi_{1,j} k_{T,e}}{T_h} \nabla T_h \right) \cdot \nabla \varphi_{1,i} d\mathbf{x} - \int_{\Gamma} \frac{\partial \mathcal{N}}{\partial c_e} \varphi_{1,j} \varphi_{1,i} \mathrm{d}s \tag{4.9}$$

Note that we are doing a full Newton on the system including for the interface integrals. This means that when we are calculating the interface integral in some element we must account for the fact that there are also non-zero test functions along the interface in the neighbouring subdomain. This gives us the coupling in the matrix between the different regions for the concentration and the potential. Specifically the coupling comes when we differentiate a function from a region with respect to an unknown from an other region. This is also shown in Appendix A.

4.4 BiCGSTAB

Notice that on each step of the Newton method we have to solve a linear system of equations. However due to the presence of first order terms and nonlinear coefficients the matrix of this system is not symmetric. It is obvious for example in Equation 4.9 that $\frac{\partial \mathbf{F}_{1,i}}{\partial C_j^l} \neq \frac{\partial \mathbf{F}_{1,j}}{\partial C_i^l}$. This means that we can't use the standart conjugate gradient method. Instead we will use the stabilized version of the biconjugate gradient, known as BiCGSTAB developed by H.A. van der Voorst [21]. If we consider a linear system of equations $\mathbf{Ax} = \mathbf{b}$, the algorithm for the preconditioned BiCGSTAB is given by [22]:

- pick $\mathbf{x}_0$
- $\mathbf{r}_0 = \mathbf{b} - \mathbf{A}\mathbf{x}_0$
- choose $\widetilde{\mathbf{r}} = \mathbf{r}_0$
- for $i = 1, 2, \ldots$

  1. $\rho_{i-1} = \widetilde{\mathbf{r}}^T \mathbf{r}_{i-1}$
     if $\rho_{i-1} = 0$ method fails
  2. if $i = 1$
     $\mathbf{p}_i = \mathbf{r}_{i-1}$
     else
     $\beta_{i-1} = (\rho_{i-1}/\rho_{i-2})(\alpha_{i-1}/\omega_{i-1})$
     $\mathbf{p}_i = \mathbf{r}_{i-1} + \beta_{i-1}(\mathbf{p}_{i-1} - \omega_{i-1}\nu_i)$
     endif
  3. $\hat{\mathbf{p}} = \mathbf{K}^{-1}\mathbf{p}_i$
  4. $\nu_i = \mathbf{A}\hat{\mathbf{p}}$
  5. $\alpha_i = \rho_{i-1}/(\widetilde{\mathbf{r}}^T \nu_i)$
  6. $\mathbf{s} = \mathbf{r}_{i-1} - \alpha_i \nu_i$
  7. if $||\mathbf{s}||$ is small enough
     $\mathbf{x}_i = \mathbf{x}_{i-1} + \alpha_i \hat{\mathbf{p}}$ and quit
  8. $\hat{\mathbf{s}} = \mathbf{K}^{-1}\mathbf{s}$
  9. $\mathbf{t} = \mathbf{A}\hat{\mathbf{s}}$
  10. $\omega_i = \mathbf{t}^T\mathbf{s}/\mathbf{t}^T\mathbf{t}$
  11. $\mathbf{x}_i = \mathbf{x}_{i-1} + \alpha_i \hat{\mathbf{p}} + \omega_i \hat{\mathbf{s}}$ if $\mathbf{x}_i$ is accurate enough quit
  12. $\mathbf{r}_i = \mathbf{s} - \omega_i \mathbf{t}$

  end

In the above algorithm $\mathbf{K}$ is the preconditioning matrix. We use it to reduce the number of iterations needed to converge to a solution. We will use the $ILUT(p, \tau)$ precoditioner as described in [20]. In it we search for an approximation of the LU factorization of the matrix $\mathbf{A}$. Specifically we start computing the factorization and we keep at most p elements on each row and throw out any element which is below the threshold defined by τ. We remind that a system with LU factorized matrix is easy to solve.
In our simulations we use $p = 20, \tau = 10^{-20}$ and for the stopping criterion we use
$(\mathbf{r}_i, \mathbf{r}_i) < (\mathbf{r}_0, \mathbf{r}_0) * tol^2$ where $tol = 10^{-12}$

5 Numerical experiments

In this section we present numerical simulations in different settings. First, in Section 5.1, we consider a single domain in which we test our solver against known functions. In Section 5.2 we consider numerical experiments for the isothermal model and in Section 5.3 we run simulations for the thermodynamic model described in Section 2. In both Section 5.2 and Section 5.3 we start with the simplest possible geometry with single electrode domains and then we continue with more complex examples. For the numerical integration in all the experiments we use a quadrature formula which is exact for polynomials of order two.

5.1 Verification of the methods

All verifications are in the same setup. Our solution domain is the unit square: $\Omega = [0,1] \times [0,1]$. Such a setting is representative of either the active particles or the electrolyte filler. Since we want to test the theoretical error estimates for the Finite Element Method and the Backward Euler Method we will use known functions. An appropriate right hand side will be introduced in each of the equations. It will be calculated by substituting the known functions in the differential operators. These problems are meant to show that the methods we use for discretization and solution are sound. The $L^2(\Omega)$ error between the known functions and their approximations will be calculated as

$$||u - u_h||^2_{L^2(\Omega)} = \int_\Omega (u - u_h)^2 \mathrm{d}\mathbf{x} = \sum_{e_k} \int_{e_k} (u - u_h)^2 \mathrm{d}\mathbf{x} \tag{5.1}$$

5.1.1 Linear problem in active particles

In our first test case the model is completely linear. This is done to show that the solver is working according to theoretical estimates. This setting is also similar to the equations in the active particles. The system still consists of three equations. All of the three equations have the following form

$$\frac{\partial u}{\partial t} - \Delta u = f(\mathbf{x}, t) \tag{5.2}$$

The functions are chosen in such a way as to test multiple cases. The first unknown function is linear to show that the approximation is indeed exact for linear functions. The second function is linear only in time. The third function is non-linear both in space and time.

$$\begin{aligned} c(\mathbf{x}, t) &= t + x_1 + x_2 \\ p(\mathbf{x}, t) &= te^{x_1 x_2} \\ T(\mathbf{x}, t) &= \sin(t x_1 x_2) \end{aligned}$$

The right hand side functions are $f_1(\mathbf{x}, t) = 1$, $f_2(\mathbf{x}, t) = e^{x_1 x_2} - te^{x_1 x_2}(x_1^2 + x_2^2)$ and $f_3 = (\mathbf{x}, t) = x_1 x_2 \cos(x_1 x_2 t) + t^2 \sin(t x_1 x_2)(x_1^2 + x_2^2)$, respectively. We use Dirichlet BC. The results of the simulation are in Table 5.1, Table 5.2 and Table 5.3. As can be seen the linear problem is solved within numerical precision and for the other two problems we get convergence of order $O(\tau + h^2)$ when we use finer meshes and smaller time steps. Due to the accumulation of computational errors in the various numerical methods it can be observed in Table 5.1 that for linear solutions smaller errors are actually achieved with coarser meshes.

Table 5.1: L^2 error for a linear differential operator for the solution $t + x_1 + x_2$ in successive meshes for t=10

	h	nodes	τ	L^2 Error
h, τ	0.27951	44	1	$1.39486392121 \times 10^{-14}$
h/2, $\tau/4$	0.13676	178	0.25	$1.91137428834 \times 10^{-13}$
h/4, $\tau/16$	0.072326	687	0.0625	$5.76361797486 \times 10^{-13}$

Table 5.2: L^2 error for a linear differential operator for the solution $te^{x_1 x_2}$ in successive meshes for t=10

	h	nodes	τ	L^2 Error	Decrease of L^2 Error
h, τ	0.27951	44	1	0.05415877155707	-
h/2, $\tau/4$	0.13676	178	0.25	0.01284746004483	4.22 times
h/4, $\tau/16$	0.072326	687	0.0625	0.002958988598254	4.34 times

Table 5.3: L^2 error for a linear differential operator for the solution $\sin(tx_1x_2)$ in successive meshes for t=10

	h	nodes	τ	L^2 Error	Decrease of L^2 Error
h, τ	0.27951	44	1	0.1435623109492	-
h/2, $\tau/4$	0.13676	178	0.25	0.04101667795240	3.5 times
h/4, $\tau/16$	0.072326	687	0.0625	0.009084416868669	4.5 times

5.1.2 Non-linear problem in electrolyte

The problem that we solve in this section can be seen as represantative of the original problem in the electrolyte. The differential operator is nonlinear and the boundary conditions are Dirichlet. With this example we test if the solver also works for non-linear problems. There are no universal theoretical error estimates in this case. We choose the following functions:

$$\begin{aligned} c(\mathbf{x},t) &= tx_1x_2 + 1 \\ p(\mathbf{x},t) &= t^2 + x_1^2 + x_2^2 + 1 \\ T(\mathbf{x},t) &= (t+1)^{x_1x_2} \end{aligned}$$

The concrete form of the considered system is:

$$\begin{aligned} \frac{\partial c}{\partial t} - \nabla \cdot \left[(c+10)^2\nabla c + (c+p)\nabla p + \frac{c}{T}\nabla T\right] &= f_1(\mathbf{x},t) \\ \frac{\partial p}{\partial t} - \nabla \cdot \left[(c+p)\nabla c + (p+10)^2\nabla p + \log(c)\nabla T\right] &= f_2(\mathbf{x},t) \\ \frac{\partial T}{\partial t} - \nabla \cdot (\nabla T) &= f_3(\mathbf{x},t) \end{aligned}$$

where

$$\begin{aligned} f_1(\mathbf{x},t) &= x_1x_2 - \big[2t^2(tx_1x_2+11)(x_1^2+x_2^2) + 4t^2 + \\ &+8(x_1^2+x_2^2+tx_1x_2+1) + t\log(t+1)(x_1^2+x_2^2)\big] \\ f_2(\mathbf{x},t) &= t^2 + x_1^2 + x_2^2 + 1 \\ f_3(\mathbf{x},t) &= 2t - \big[4tx_1x_2 + t^2(x_1^2+x_2^2) + 4(t^2+x_1^2+x_2^2+6)^2 + \\ &+ 8(t^2+x_1^2+x_2^2+6)(x_1^2+x_2^2) + \\ &(t+1)^{x_1x_2}\log(t+1)(x_1^2+x_2^2)\left(\frac{t}{tx_1x_2+1} + \log(t+1)\log(tx_1x_2+1)\right)\Big] \end{aligned}$$

and the functions themselves are imposed as Dirichlet boundary conditions. As can be seen from Table 5.4, Table 5.5 and Table 5.6 we still have convergence and even the order $O(\tau + h^2)$ is preserved.

Table 5.4: L^2 error for a non-linear differential operator for the solution $tx_1x_2 + 1$ in successive meshes for t=0.16

	h	nodes	τ	L^2 Error	Decrease of L^2 Error
h, τ	0.38845	27	0.04	0.00082815717534	-
h/2, τ/4	0.19186	98	0.01	0.000148208283622	5.58 times
h/4, τ/16	0.096785	351	0.0025	$3.4104740058\times10^{-5}$	4.34 times

Table 5.5: L^2 error for a non-linear differential operator for the solution $t^2 + x_1^2 + x_2^2 + 1$ in successive meshes for t=0.16

	h	nodes	τ	L^2 Error	Decrease of L^2 Error
h, τ	0.38845	27	0.04	0.02110775794042	-
h/2, τ/4	0.19186	98	0.01	0.004584480029279	4.6 times
h/4, τ/16	0.096785	351	0.0025	0.00112427933167	4.07 times

Table 5.6: L^2 error for a non-linear differential operator for the solution $(t+1)^{x_1x_2}$ in successive meshes for t=0.16

	h	nodes	τ	L^2 Error	Decrease of L^2 Error
h, τ	0.38845	27	0.04	0.000821360244424	-
h/2, τ/4	0.19186	98	0.01	0.000151007630003	5.44 times
h/4, τ/16	0.096785	351	0.0025	$3.53157998497\times10^{-5}$	4.27 times

5.1.3 Interface problem

In this section we present a simple interface problem. We test the accuracy for such problems with the methods that we use. The differential operator is the same as in Section 5.1.1, i.e. linear. There are interface conditions however, dependent on the values of the discontinuous function on both sides of the interface. The function we use is:

$$u = u_1 = 5e^{x_1 - t} + 2t, \quad \mathbf{x} \in \Omega_1 \tag{5.3a}$$

$$u = u_2 = 5e^{x_1 - t} + t, \quad \mathbf{x} \in \Omega_2 \tag{5.3b}$$

The domain Ω is again the unit square. It is split into two equal subdomains $\Omega_1 = [0, 0.5] \times [0, 1]$ and $\Omega_2 = [0.5, 1] \times [0, 1]$.

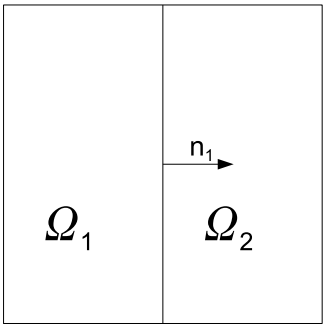

Figure 9: The solution domain for example 5.1.3

The interface condition which we use is:

$$\frac{\partial u_1}{\partial \mathbf{n_1}} = \frac{\partial u_2}{\partial \mathbf{n_1}} = 2u_2 - u_1 \tag{5.4}$$

The right hand side is

$$f(\mathbf{x},t) = -10e^{x_1-t} + 2, \quad \mathbf{x} \in \Omega_1 \tag{5.5}$$
$$f(\mathbf{x},t) = -10e^{x_1-t} + 1, \quad \mathbf{x} \in \Omega_2 \tag{5.6}$$

We also use the following boundary conditions:

$$u(\mathbf{x},t) = 5e^{-t} + 2t, \quad \mathbf{x} \in \{x_1 = 0\} \tag{5.7}$$
$$\frac{\partial u}{\partial \mathbf{n}} = 0, \quad \mathbf{x} \in \{x_2 = 0 \cup x_2 = 1\} \tag{5.8}$$
$$\frac{\partial u}{\partial \mathbf{n}} = 5e^{x_1-t}, \quad \mathbf{x} \in \{x_1 = 1\} \tag{5.9}$$
$$\tag{5.10}$$

As can be observed in Table 5.7 we again achieve $O(\tau + h^2)$ convergence rate.

Table 5.7: L^2 error for an interface problem with linear differential operator for a discontinuous function in successive meshes for t=1.2

	h	nodes	τ	L^2 Error	Decrease of L^2 Error
h, τ	0.17678	119	0.4	0.3233774211799044	-
h/2, $\tau/4$	0.088394	438	0.1	0.08601145571864255	3.76 times
h/4, $\tau/16$	0.045423	1693	0.025	0.02182305173126918	3.94 times
h/8, $\tau/64$	0.022429	6550	0.00625	0.005476552385904158	3.98 times

5.2 Simulations on the isothermal model

Here we run simulations for the isothermal model. The initial and boundary conditions that we impose are specified in the first example in Section 5.2.1 where we have plate electrodes.
The parameters that we use in our numerical experiments are given in Table 5.8. We run our simulations for time $t = 4058$s and as we can see from the figures below, we obtain reasonable physical results.

Table 5.8: Values of the parameters used for the simulations

	$D\left[\frac{\text{cm}^2}{\text{s}}\right]$	t_+	$\kappa\left[\frac{\text{S}}{\text{cm}}\right]$	$c_{max}\left[\frac{\text{mol}}{\text{cm}^3}\right]$
Electrolyte	7.5×10^{-7}	0.363	0.002	
Cathode	1.0×10^{-9}	0	0.038	0.02286
Anode	3.9×10^{-10}	0	1.0	0.02639

Table 5.9: Values of the parameters for the interface conditions

α_a	α_c	$k\left[\frac{\text{A}}{\text{cm}^2}\right]$
0.5	0.5	0.2

Finally for U_0 we have

$$U_0 = -0.132 + 1.41e^{-3.52soc}, \mathbf{x} \in \Omega_a \tag{5.11a}$$
$$U_0 = 4.06279 + 0.0677504\tanh(-21.8502soc + 12.8268) - 0.045e^{-71.69soc^8} - 0.105734\left(\frac{1}{(1.00167 - soc)^{0.379571}} - 1.576\right) + 0.01e^{-200(soc-0.19)}, \mathbf{x} \in \Omega_c \tag{5.11b}$$

5.2.1 Plates

Here we have electrolyte between one anode and one cathode plate as shown in Figure 10.

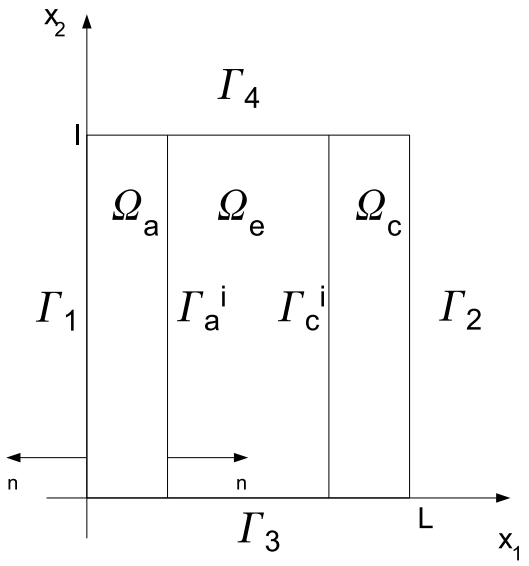

Figure 10: Simple layered battery model domain

The following initial and boundary conditions are imposed:
Initial conditions: t=0:

Table 5.10: Initial concentration

	$c_0 \left[\frac{\text{mol}}{\text{cm}^3}\right]$
electrolyte	0.001
anode	$0.2c_{max} = 0.005278$
cathode	$0.8c_{max} = 0.018288$

Table 5.11: Initial potential

	ϕ_0[V]
electrolyte	0
anode	$U_0(c_{0,a}) = 0.5654$
cathode	$U_0(c_{0,c}) = 3.9675$

where $U_0(c)$ is the open circuit potential, a given function of the concentration of Li-ions $c(x,t)$.
Boundary conditions:
Dirichlet boundary conditions:

$$\Gamma_1 : \quad \phi|_{\Gamma_1} = U_0(c_{0,a})|_{anode} = 0.5654 \tag{5.12}$$

Neumann boundary conditions:

$$\Gamma_1 \cup \Gamma_2 : \quad (\nabla c \cdot \mathbf{n})\,|_{\Gamma_1 \cup \Gamma_2} = 0 \tag{5.13}$$

$$\Gamma_2 : \quad (k_{22}\nabla\phi \cdot \mathbf{n})\,|_{\Gamma_2} = E_2 = const = 0.0005 \tag{5.14}$$

$$\Gamma_3 \cup \Gamma_4 : \quad (\mathbf{N} \cdot \mathbf{n})\,|_{\Gamma_3 \cup \Gamma_4} = (\mathbf{J} \cdot \mathbf{n})\,|_{\Gamma_3 \cup \Gamma_4} = 0 \tag{5.15}$$

Also, in all the successive simulations, on the interface Γ_a^i and Γ_c^i we impose the interface conditions.
We ran simulations for time $t = 1000$s. As we can see from Table 5.10 the initial concentration of Li-ions in the cathode is $0.018288\frac{mol}{cm^3}$ and is bigger than that in the anode which is $0.005278\frac{mol}{cm^3}$. Hence, due to the applied electrical current on Γ_2 which is the cathode exterior boundary, the Li-ions move from the cathode to the anode. This means that we simulate charging of the battery. Therefore in the end of the simulations the concentration in the cathode decreases approximately to $0.01760\frac{mol}{cm^3}$, while that in the anode increases to $0.007\frac{mol}{cm^3}$ as shown in Figure 11.
At time $t = 1000$s, as we can see from from Figure 12a, the value of the potential in the anode is still 0.5654V, i.e. they do not change and is the same as that at time $t = 0$. This result was expected because we imposed a Dirichlet boundary condition (5.12) on the anode exterior boundary Γ_1. On the other hand, the potential in the cathode slightly increases from 3.9675V to 4.0964V (see Figure 12b), and also the potential in the electrolty increases from 0V to 0.0985V (see Figure 12).
Another thing that we can observe is that when we apply bigger electrical current on Γ_2 (see Figure 13b), taking $E_2 = 0.005$, the process of Li-ions moving from the region with bigger concentration-the cathode to the region with smaller concetration-the anode is getting faster. In this case the potential in the cathode increases significantly form 3.9675V at time $t = 0$ to 4.8113V at time $t = 1000$s. As we can see from Figure 13a the potential in the electrolyte also increases from 0V at time $t = 0$ to 0.585V at time $t = 1000$s.
Judging by the numerical experiments, we can conclude that the obtained results from the simulations coincide with the expected physical phenomena.

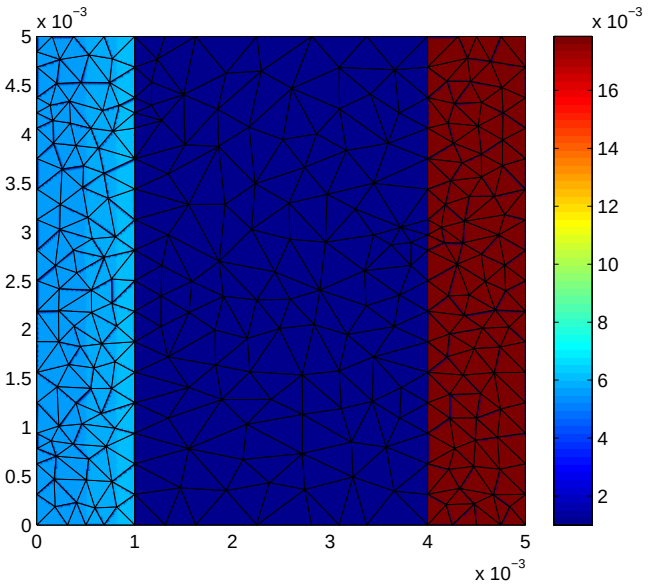

Figure 11: Concentration at time 1000s

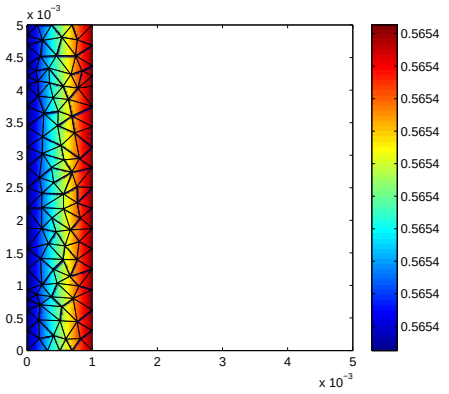

(a) Potential in Anode at time 1000s

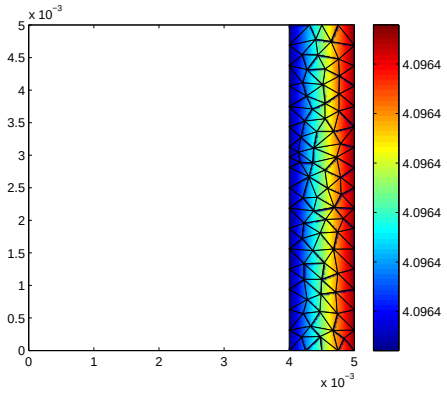

(b) Potential in Cathode at time 1000s

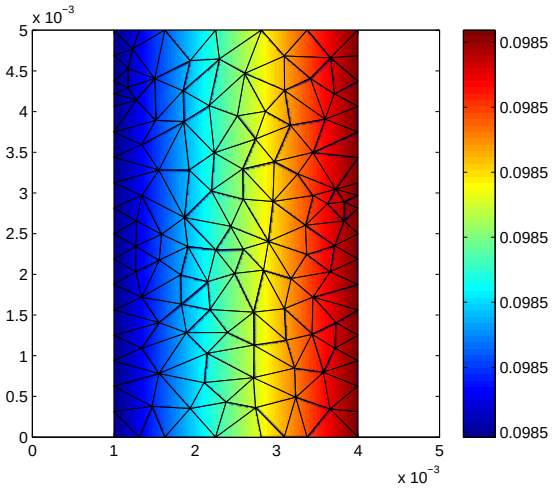

Figure 12: Potential in Electrolyte at time 1000s

Here we show the simulations with the higher electrical current applied on the cathode:

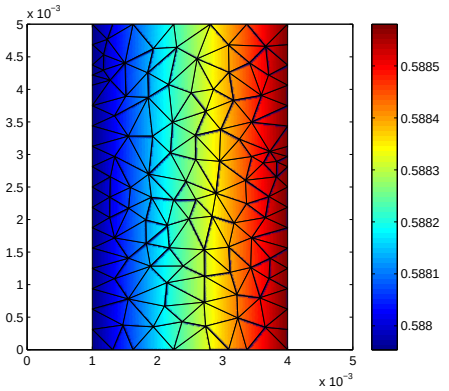

(a) Steep Potential in the Electrolyte at time 1000s

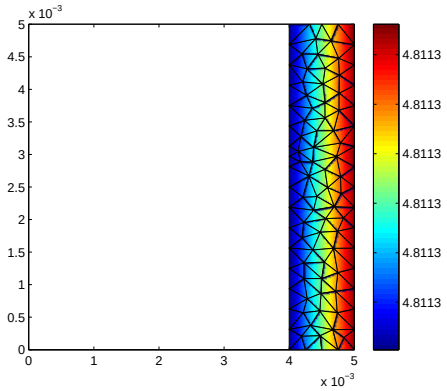

(b) Steep Potential in the Cathode at time 1000s

5.2.2 Electrolyte with five anode active particles and four cathode active particles

Here we show numerical results for a Li-ion battery cell with five anode active particles and four cathode active particles. For this example instead of charging, we are discharging the battery. Hence the applied current is on Γ_1 instead of on Γ_2 and the ions move from the anode (where their concentration is higher) to the cathode. Moreover the initial values for the concentration in the particles are $0.69999 * c_{max_{anode}}$ for the anode and $0.30001 * c_{max_{cathode}}$ for the cathode. Again our numerical results seem physically correct.

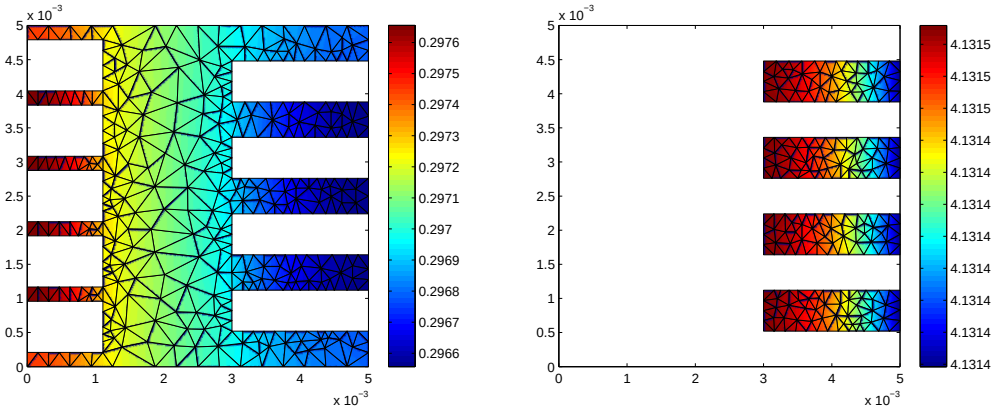

(c) Potential in Electrolyte at time 3617s

(d) Potential in Cathode at time 3617s

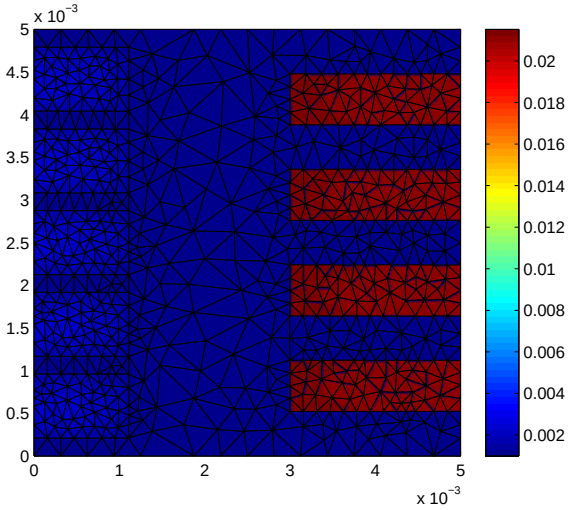

Figure 13: Concentration at time 3617s

5.3 Simulations on the thermodynamic model

In this section we present numerical simulations in different settings. The linear systems of equations in this section were solved not with the BiCGSTAB solver but with the commercial SAMG solver. We show simulations of charging and discharging of a battery. We vary the strength of the applied current to show its effect on the temperature. We also vary the thermoconductivity of the boundary. The total area of the particles in the anode and in the cathode is chosen in such a way that the maximum number of Lithium ions that can be stored in each electrode is the same. The parameters that we use in our numerical experiments are given in Table 5.12. We run our simulations for time $t = 2500$s.

Table 5.12: Values of the parameters used for the simulations

	$D\left[\frac{\text{cm}^2}{\text{s}}\right]$	t_+	$\kappa\left[\frac{\text{S}}{\text{cm}}\right]$	k_T	$\lambda\left[\frac{\text{W}}{\text{cm}\cdot\text{K}}\right]$	$\rho\left[\frac{\text{kg}}{\text{cm}^3}\right]$	$c_p\left[\frac{\text{J}}{\text{kg}\cdot\text{K}}\right]$	$c_{max}\left[\frac{\text{mol}}{\text{cm}^3}\right]$
Electrolyte	7.5×10^{-7}	0.363	0.002	1	0.01	0.001	2000	
Cathode	1.0×10^{-9}	0	0.038	1	0.01	0.0036	7000	0.023671
Anode	3.9×10^{-10}	0	1.0	1	0.01	0.0029	7000	0.024681

Table 5.13: Values of the parameters for the interface conditions

α_a	α_c	$k_{anode}\left[\frac{\text{A}}{\text{cm}^2}\right]$	$k_{cathode}\left[\frac{\text{A}}{\text{cm}^2}\right]$	Π_{anode}	$\Pi_{cathode}$
0.5	0.5	0.002	0.2	-0.28	-0.38

Finally for U_0 we use

$$U_0 = -0.132 + 1.41e^{-3.52\text{soc}}, \mathbf{x} \in \Omega_a \tag{5.16a}$$

$$U_0 = 4.06279 + 0.0677504\tanh(-21.8502\text{soc} + 12.8268) - 0.045e^{-71.69\text{soc}^8} - 0.105734\left(\frac{1}{(1.00167 - \text{soc})^{0.379571}} - 1.576\right) + 0.01e^{-200(\text{soc}-0.19)}, \mathbf{x} \in \Omega_c \tag{5.16b}$$

where $\text{soc} = c_s/c_{s,max}$. The setting of the problem is on the microscale level as described in Section 2. We have $\Omega = [0, 5 \times 10^{-3}] \times [0, 5 \times 10^{-3}]$ and the units are in centimeters.

Table 5.14: Initial values for the charging process

	$c\left[\frac{\text{mol}}{\text{cm}^3}\right]$	Φ[V]	T[K]
Electrolyte	0.001	0	300
Cathode	0.0213	4	300
Anode	0.0025	0.8596	300

Table 5.15: Initial values for the discharging process

	$c\left[\frac{\text{mol}}{\text{cm}^3}\right]$	Φ[V]	T[K]
Electrolyte	0.001	0	300
Cathode	0.0083	4.13	300
Anode	0.016	0.011	300

For the boundary conditions we use:

$$\Phi(\mathbf{x}, t) = 0.8596\text{V}, \quad \mathbf{x} \in \partial\Omega_{anode,outer} \tag{5.17}$$

$$\sigma\frac{\partial\Phi}{\partial\mathbf{n}} = i_{appl}\frac{\text{A}}{\text{cm}^2}, \quad \mathbf{x} \in \partial\Omega_{cathode,outer} \tag{5.18}$$

$$\lambda\frac{\partial T}{\partial\mathbf{n}} = \alpha \times (T_{outer} - T), \quad \mathbf{x} \in \partial\Omega \tag{5.19}$$

for the charging process and

$$\Phi(\mathbf{x}, t) = 0.011\text{V}, \quad \mathbf{x} \in \partial\Omega_{anode,outer} \tag{5.20}$$

$$\sigma\frac{\partial\Phi}{\partial\mathbf{n}} = i_{appl}\frac{\text{A}}{\text{cm}^2}, \quad \mathbf{x} \in \partial\Omega_{cathode,outer} \tag{5.21}$$

$$\lambda\frac{\partial T}{\partial\mathbf{n}} = \alpha \times (T_{outer} - T), \quad \mathbf{x} \in \partial\Omega \tag{5.22}$$

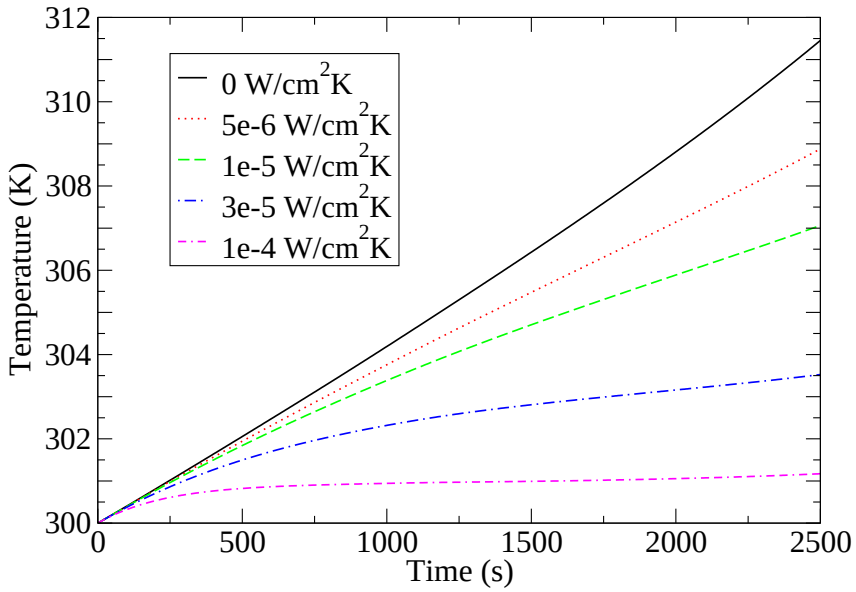

Figure 14: Evolution of the temperature in a battery cell during discharge for 2500s for applied current density 10^{-3} A/cm^2 for different values of α.

for the discharging process. $T_{outer} = 300K$ is the ambient temperature. We also take $\alpha = \{0$ W/cm^{2}K, 5×10^{-6} W/cm^{2}K, 10^{-5} W/cm^{2}K, 3×10^{-5} W/cm^{2}K, 10^{-4} W/cm^{2}K$\}$ in each case in order to test different levels of thermal insulation for the battery and $i_{appl} = \{5 \times 10^{-4}A/cm^2, 10^{-3}A/cm^2\}$ in order to observe what happens when we drive different currents through the battery. The rest of the boundary conditions have been already defined in Section 2. For our problem the values of the temperature are practically uniform at each time step hence we show only its evolution and not its distribution in the battery. It is obvious from the figures that when driving stronger currents the temperature increases faster, as was expected. The behavior of the concentration was not influenced by the temperature in this test case since the gradient is practically zero. Simulation snapshots for the concentration at $t = 2000$ seconds are shown for charge and discharge for $\alpha = 0$ in Figure 18 and Figure 19 respectively. There are two scales - one for the concentration in the electrolyte and one for the concentration in the active particles.

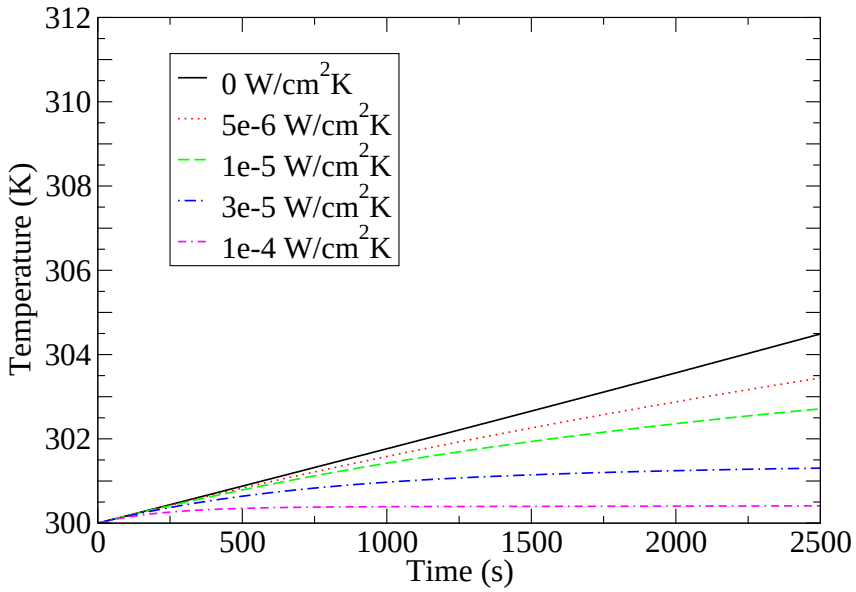

Figure 15: Evolution of the temperature in a battery cell during discharge for 2500s for applied current density 5×10^{-4} A/cm^2 for different values of α.

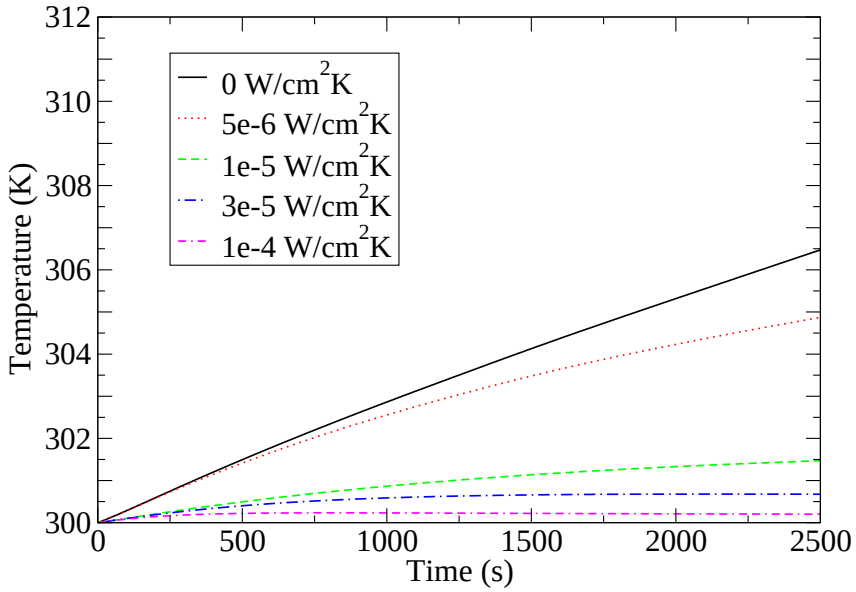

Figure 16: Evolution of the temperature in a battery cell during charge for 2500s for applied current density 10^{-3} A/cm^2 for different values of α.

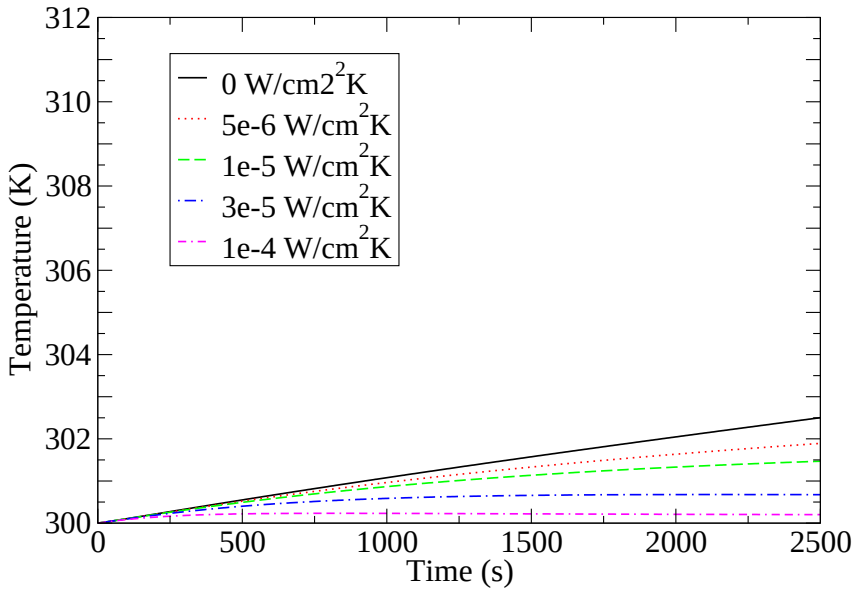

Figure 17: Evolution of the temperature in a battery cell during charge for 2500s for applied current density 5×10^{-4} A/cm^2 for different values of α.

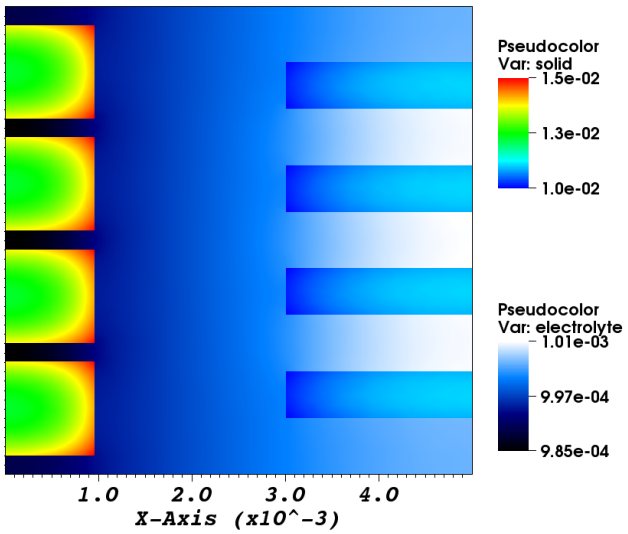

Figure 18: Spatial profile of the lithium concentration (mol/cm^3) in a battery cell after 2000s of charging for applied current density 10^{-3} A/cm^2.

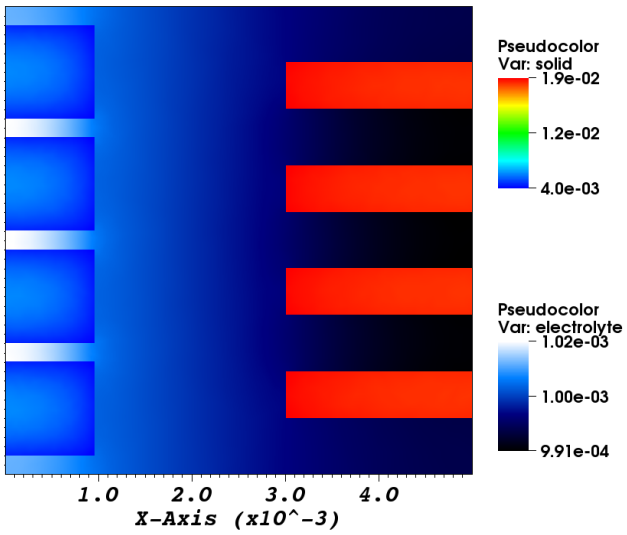

Figure 19: Spatial profile of the lithium concentration (mol/cm^3) in a battery cell after 2000s of discharging for applied current density 10^{-3} A/cm^2

6 Conclusion

We have successfully developed a solver for the cell resolved thermodynamic model of a lithium ion battery from [10] in a two dimensional setting. The results obtained from the simulations seem physically correct. The node splitting technique that we used for the finite element method allowed us to correctly simulate the discontinuous quantities.

A natural extension of our solver would be to move it to a realistic three dimensional setting. In its current form the geometry does not allow to have the complicated structures observed in real batteries. The added complexity of the increased number of unknowns will also bring the need for better preconditioners and parallel implementations. To ensure the conservation of physical laws nonconforming elements would also have to be included. If the model is extended to include the degradation processes for the particles, which may include changing their geometry, the mesh should allow for modification. Higher order time discretization methods may also be implemented.

A Derivatives

In this appendix we present some of the derivatives needed in the Newton method. Instead of writing the approximating functions as linear combinations we use the already introduced lower h notation, i.e. c_h, P_h, T_h. For clarity we first present their derivatives

$$\frac{\partial c_h}{\partial C_j} = \varphi_{1,j} \tag{A.1a}$$

$$\frac{\partial P_h}{\partial P_j} = \varphi_{2,j} \tag{A.1b}$$

$$\frac{\partial T_h}{\partial T_j} = \varphi_{3,j} \tag{A.1c}$$

For completeness we also show the derivative calculated in Section 4.3. We begin with the derivatives of the three equations in the electrolyte differentiated with respect to C_j^l:

$$\begin{aligned}\frac{\partial \mathbf{F}_{1,i}}{\partial C_j^l} =& \int_{\Omega_e} \frac{\varphi_{1,j}}{\tau}\varphi_{1,i}\mathrm{d}\mathbf{x} - \int_{\partial\Omega_{e,outer}} \left(\frac{D_e\varphi_{1,j}k_{T,e}}{T_h} - \kappa\frac{t_+R\varphi_{1,j}}{F^2c_h}\right) g(T_h)\varphi_{1,i}\mathrm{d}s + \\ & \int_{\Omega_e} \left(D_e\nabla\varphi_{1,j} - \frac{t_+}{F}\frac{\partial \mathbf{j}_e}{\partial c_e} + \frac{D_e\varphi_{1,j}k_{T,e}}{T_h}\nabla T_h\right)\cdot\nabla\varphi_{1,i}d\mathbf{x} - \int_\Gamma \frac{\partial \mathcal{N}}{\partial c_e}\varphi_{1,j}\varphi_{1,i}\mathrm{d}s\end{aligned} \tag{A.2a}$$

$$\begin{aligned}\frac{\partial \mathbf{F}_{2,i}}{\partial C_j^l} =& \int_{\Omega_e} \left(\frac{\kappa(1-t_+)RT_h}{F}\left(\frac{\varphi_{1,j}}{c_h^2}\nabla c_h - \frac{1}{c_h}\nabla\varphi_{1,j}\right)\right)\cdot\nabla\varphi_{2,i}\mathrm{d}\mathbf{x} - \int_{\Omega_e}\left(\kappa\frac{R\varphi_{1,j}}{Fc_h}\nabla T_h\right)\cdot\nabla\varphi_{2,i}\mathrm{d}\mathbf{x} + \\ & \int_{\partial\Omega_{e,outer}} \kappa\frac{R\varphi_{1,j}}{Fc_h}g(T_h)\varphi_{2,i}\mathrm{d}s - \int_\Gamma \frac{\partial \mathcal{J}}{\partial c_e}\varphi_{1,j}\varphi_{2,i}\mathrm{d}s\end{aligned} \tag{A.2b}$$

$$\begin{aligned}\frac{\partial \mathbf{F}_{3,i}}{\partial C_j^l} =& -\int_\Omega \varphi_{3,i}2\frac{\mathbf{j}\cdot\frac{\partial \mathbf{j}}{\partial c}}{\kappa}\mathrm{d}\mathbf{x} - \int_\Omega \frac{\varphi_{3,i}}{D}\left((\mathbf{N}_+ - \frac{t_+}{F}\mathbf{j})^2\frac{\partial^2\mu}{\partial c^2}\varphi_{1,j} + 2(\mathbf{N}_+ - \frac{t_+}{F}\mathbf{j})\cdot\frac{\partial(\mathbf{N}_+ - \frac{t_+}{F}\mathbf{j})}{\partial c}\frac{\partial\mu}{\partial c}\right)\mathrm{d}\mathbf{x} - \\ & \int_\Omega \frac{k_T}{T_h}\nabla(\varphi_{3,i}T_h)\cdot\left(\varphi_{1,j}\frac{\partial\mu}{\partial c}(\mathbf{N}_+ - \frac{t_+}{F}\mathbf{j}) + c_h\frac{\partial^2\mu}{\partial c^2}\varphi_{1,j}(\mathbf{N}_+ - \frac{t_+}{F}\mathbf{j}) + c_h\frac{\partial\mu}{\partial c}\frac{\partial(\mathbf{N}_+ - \frac{t_+}{F}\mathbf{j})}{\partial c}\right)\mathrm{d}\mathbf{x} + \\ & \int_{\partial\Omega}\varphi_{3,i}k_T\left(\varphi_{1,j}\frac{\partial\mu}{\partial c}f(c_h,T_h) + c\frac{\partial^2\mu}{\partial c^2}\varphi_{1,j}f(c_h,T_h) + c\frac{\partial\mu}{\partial c}\frac{\partial f(c_h,T_h)}{\partial c}\varphi_{1,j}\right)\mathrm{d}s - \int_\Gamma \varphi_{3,i}\frac{\partial\mathcal{T}}{\partial c_e}\varphi_{3,j}\mathrm{d}s\end{aligned} \tag{A.2c}$$

Since the rest of the derivatives are done in a similar manner we do not show them here. We will calculate the derivatives of the first two equations of the model when we test with a basis function whose support is in the electrolyte and the derivative is with respect to an unknown which is from the side of an electrode. We use additional indices to differentiate them.

$$\frac{\partial \mathbf{F}_{1,i,e}}{\partial C_{j,s}^l} = -\int_\Gamma \frac{\partial\mathcal{N}}{\partial c_s}\varphi_{1,j,s}\varphi_{1,i,e}\mathrm{d}s \tag{A.3}$$

$$\frac{\partial \mathbf{F}_{2,i,e}}{\partial C_{j,s}^l} = -\int_\Gamma \frac{\partial\mathcal{J}}{\partial c_s}\varphi_{1,j,s}\varphi_{2,i,e}\mathrm{d}s \tag{A.4}$$

Since the third equation is defined on the whole of Ω and also the test functions in V_3 are continuous in the whole domain the derivative there is simply the standart derivative.

References

[1] Susanne C. Brenner and L. Ridgway Scott. *The Mathematical Theory of Finite Element Methods*. Springer, 3rd edition, 2008.

[2] M. Broussely, Ph. Biensan, F. Bonhomme, Ph. Blanchard, S. Herreyre, K. Nechev, and R.J. Staniewicz. Main aging mechanisms in li ion batteries. *Journal of Power Sources*, 146(1-2):90 – 96, 2005. Selected papers pressented at the 12th International Meeting on Lithium Batteries.

[3] Yufei Chen and J.W. Evans. Heat transfer phenomena in lithium/polymer-electrolyte batteries for electric vehicle application. *Journal of the Electrochemical Society*, 140:7, 1993.

[4] Yufei Chen and J.W. Evans. Three-dimensional thermal modeling of lithium-polymer batteries under galvanostatic discharge and dynamic power profile. *Journal of the Electrochemical Society*, 141:11, 1994.

[5] Zhangxin Chen. *Finite Element Methods and Their Applications*. Springer, 2005.

[6] C.W. Wang and A.M. Sastry. Mesoscale modeling of li-ion polymer cell. *Journal of the Electrochemical Society*, 154(11):A1035–A1047, 2007.

[7] L.C. Evans. *Partial Differential Equations*. American Mathematical Society, 1998.

[8] William C. Gear. *Numerical Initial Value Problems in Ordinary Differential Equations*. Prentice-Hall Inc., 1971.

[9] C.T. Kelley. *Solving Nonlinear Equations with Newton's Method*. SIAM, 2003.

[10] A. Latz and J. Zausch. Thermodynamic consistent transport theory of li-ion batteries. *Journal of Power Sources*, 196(6):3296 – 3302, 2011.

[11] Arnulf Latz, Jochen Zausch, and Oleg Iliev. Modeling of species and charge transport in li-ion batteries based on non-equilibrium thermodynamics. In *Proceedings of the 7th international conference on Numerical methods and applications*, NMA'10, pages 329–337, Berlin, Heidelberg, 2011. Springer-Verlag.

[12] G. B. Less, J. H. Seo, S. Han, A. M. Sastry, J. Zausch, A. Latz, S. Schmidt, C. Wieser, D. Kehrwald, and S. Fell. Micro-scale modeling of li-ion batteries: Parameterization and validation. *Journal of The Electrochemical Society*, 159(6):A697–A704, 2012.

[13] David Linden and Thomas B. Reddy. *Handbook of Batteries*. McGraw-Hill Professional, 3rd edition, 2001.

[14] John Newman and Karen E. Thomas-Alyea. *Electrochemical Systems*. Wiley-Interscience, 3rd edition, 2004.

[15] J.M. Ortega and W.C. Rheinboldt. *Iterative Solution of Nonlinear Equations in Several Variables*. SIAM, 1970.

[16] Carolyn R Pals and John Newman. Thermal modeling of the lithium/polymer battery .1. discharge behavior of a single-cell. *Journal of the Electrochemical Society*, 142(10):3274–3281, 1995.

[17] P. Popov, Y. Vutov, S. Margenov, and O. Iliev. Finite volume discretization of equations describing nonlinear diffusion in li-ion batteries. In *Proceedings of the 7th international conference on Numerical methods and applications*, NMA'10, pages 338–346, Berlin, Heidelberg, 2011. Springer-Verlag.

[18] J.N. Reddy. *An Introduction to the Finite Element Method*. McGraw-Hill, Inc., 2nd edition, 1993.

[19] Michael Renardy and Robert Rogers. *An Introduction to Partial Differential Equations*. Springer, 2nd edition, 2004.

[20] Yousef Saad. *Iterative Methods for Sparse Linear Systems*. SIAM, 2nd edition, 2003.

[21] H.A. van der Voorst. Bi-CGSTAB: A fast and smoothly converging variant of Bi-CG for the solution of nonsymmetric linear systems. *SIAM Journal on Scientific and Statistical Computing*, 13:631–644, 1992.

[22] H.A. van der Voorst. *Iterative Krylov Methods for Large Linear Systems*. Cambridge University Press, 2003.

[23] J. Vetter, P. Novk, M.R. Wagner, C. Veit, K.-C. Mller, J.O. Besenhard, M. Winter, M. Wohlfahrt-Mehrens, C. Vogler, and A. Hammouche. Ageing mechanisms in lithium-ion batteries. *Journal of Power Sources*, 147(1-2):269 – 281, 2005.

Published reports of the Fraunhofer ITWM

The PDF-files of the following reports are available under:
www.itwm.fraunhofer.de/de/zentral__berichte/berichte

1. D. Hietel, K. Steiner, J. Struckmeier
A Finite - Volume Particle Method for Compressible Flows
(19 pages, 1998)

2. M. Feldmann, S. Seibold
Damage Diagnosis of Rotors: Application of Hilbert Transform and Multi-Hypothesis Testing
Keywords: Hilbert transform, damage diagnosis, Kalman filtering, non-linear dynamics
(23 pages, 1998)

3. Y. Ben-Haim, S. Seibold
Robust Reliability of Diagnostic Multi-Hypothesis Algorithms: Application to Rotating Machinery
Keywords: Robust reliability, convex models, Kalman filtering, multi-hypothesis diagnosis, rotating machinery, crack diagnosis
(24 pages, 1998)

4. F.-Th. Lentes, N. Siedow
Three-dimensional Radiative Heat Transfer in Glass Cooling Processes
(23 pages, 1998)

5. A. Klar, R. Wegener
A hierarchy of models for multilane vehicular traffic
Part I: Modeling
(23 pages, 1998)

Part II: Numerical and stochastic investigations
(17 pages, 1998)

6. A. Klar, N. Siedow
Boundary Layers and Domain Decomposition for Radiative Heat Transfer and Diffusion Equations: Applications to Glass Manufacturing Processes
(24 pages, 1998)

7. I. Choquet
Heterogeneous catalysis modelling and numerical simulation in rarified gas flows Part I: Coverage locally at equilibrium
(24 pages, 1998)

8. J. Ohser, B. Steinbach, C. Lang
Efficient Texture Analysis of Binary Images
(17 pages, 1998)

9. J. Orlik
Homogenization for viscoelasticity of the integral type with aging and shrinkage
(20 pages, 1998)

10. J. Mohring
Helmholtz Resonators with Large Aperture
(21 pages, 1998)

11. H. W. Hamacher, A. Schöbel
On Center Cycles in Grid Graphs
(15 pages, 1998)

12. H. W. Hamacher, K.-H. Küfer
Inverse radiation therapy planning - a multiple objective optimisation approach
(14 pages, 1999)

13. C. Lang, J. Ohser, R. Hilfer
On the Analysis of Spatial Binary Images
(20 pages, 1999)

14. M. Junk
On the Construction of Discrete Equilibrium Distributions for Kinetic Schemes
(24 pages, 1999)

15. M. Junk, S. V. Raghurame Rao
A new discrete velocity method for Navier-Stokes equations
(20 pages, 1999)

16. H. Neunzert
Mathematics as a Key to Key Technologies
(39 pages, 1999)

17. J. Ohser, K. Sandau
Considerations about the Estimation of the Size Distribution in Wicksell's Corpuscle Problem
(18 pages, 1999)

18. E. Carrizosa, H. W. Hamacher, R. Klein, S. Nickel
Solving nonconvex planar location problems by finite dominating sets
Keywords: Continuous Location, Polyhedral Gauges, Finite Dominating Sets, Approximation, Sandwich Algorithm, Greedy Algorithm
(19 pages, 2000)

19. A. Becker
A Review on Image Distortion Measures
Keywords: Distortion measure, human visual system
(26 pages, 2000)

20. H. W. Hamacher, M. Labbé, S. Nickel, T. Sonneborn
Polyhedral Properties of the Uncapacitated Multiple Allocation Hub Location Problem
Keywords: integer programming, hub location, facility location, valid inequalities, facets, branch and cut
(21 pages, 2000)

21. H. W. Hamacher, A. Schöbel
Design of Zone Tariff Systems in Public Transportation
(30 pages, 2001)

22. D. Hietel, M. Junk, R. Keck, D. Teleaga
The Finite-Volume-Particle Method for Conservation Laws
(16 pages, 2001)

23. T. Bender, H. Hennes, J. Kalcsics, M. T. Melo, S. Nickel
Location Software and Interface with GIS and Supply Chain Management
Keywords: facility location, software development, geographical information systems, supply chain management
(48 pages, 2001)

24. H. W. Hamacher, S. A. Tjandra
Mathematical Modelling of Evacuation Problems: A State of Art
(44 pages, 2001)

25. J. Kuhnert, S. Tiwari
Grid free method for solving the Poisson equation
Keywords: Poisson equation, Least squares method, Grid free method
(19 pages, 2001)

26. T. Götz, H. Rave, D. Reinel-Bitzer, K. Steiner, H. Tiemeier
Simulation of the fiber spinning process
Keywords: Melt spinning, fiber model, Lattice Boltzmann, CFD
(19 pages, 2001)

27. A. Zemitis
On interaction of a liquid film with an obstacle
Keywords: impinging jets, liquid film, models, numerical solution, shape
(22 pages, 2001)

28. I. Ginzburg, K. Steiner
Free surface lattice-Boltzmann method to model the filling of expanding cavities by Bingham Fluids
Keywords: Generalized LBE, free-surface phenomena, interface boundary conditions, filling processes, Bingham viscoplastic model, regularized models
(22 pages, 2001)

29. H. Neunzert
»Denn nichts ist für den Menschen als Menschen etwas wert, was er nicht mit Leidenschaft tun kann«
Vortrag anlässlich der Verleihung des Akademiepreises des Landes Rheinland-Pfalz am 21.11.2001
Keywords: Lehre, Forschung, angewandte Mathematik, Mehrskalenanalyse, Strömungsmechanik
(18 pages, 2001)

30. J. Kuhnert, S. Tiwari
Finite pointset method based on the projection method for simulations of the incompressible Navier-Stokes equations
Keywords: Incompressible Navier-Stokes equations, Meshfree method, Projection method, Particle scheme, Least squares approximation
AMS subject classification: 76D05, 76M28
(25 pages, 2001)

31. R. Korn, M. Krekel
Optimal Portfolios with Fixed Consumption or Income Streams
Keywords: Portfolio optimisation, stochastic control, HJB equation, discretisation of control problems
(23 pages, 2002)

32. M. Krekel
Optimal portfolios with a loan dependent credit spread
Keywords: Portfolio optimisation, stochastic control, HJB equation, credit spread, log utility, power utility, non-linear wealth dynamics
(25 pages, 2002)

33. J. Ohser, W. Nagel, K. Schladitz
The Euler number of discretized sets – on the choice of adjacency in homogeneous lattices
Keywords: image analysis, Euler number, neighborhod relationships, cuboidal lattice
(32 pages, 2002)

34. I. Ginzburg, K. Steiner
Lattice Boltzmann Model for Free-Surface flow and Its Application to Filling Process in Casting
Keywords: Lattice Boltzmann models; free-surface phenomena; interface boundary conditions; filling processes; injection molding; volume of fluid method; interface boundary conditions; advection-schemes; upwind-schemes
(54 pages, 2002)

35. M. Günther, A. Klar, T. Materne, R. Wegener
Multivalued fundamental diagrams and stop and go waves for continuum traffic equations
Keywords: traffic flow, macroscopic equations, kinetic derivation, multivalued fundamental diagram, stop and go waves, phase transitions
(25 pages, 2002)

36. S. Feldmann, P. Lang, D. Prätzel-Wolters
Parameter influence on the zeros of network determinants
Keywords: Networks, Equicofactor matrix polynomials, Realization theory, Matrix perturbation theory
(30 pages, 2002)

37. K. Koch, J. Ohser, K. Schladitz
Spectral theory for random closed sets and estimating the covariance via frequency space
Keywords: Random set, Bartlett spectrum, fast Fourier transform, power spectrum
(28 pages, 2002)

38. D. d'Humières, I. Ginzburg
Multi-reflection boundary conditions for lattice Boltzmann models
Keywords: lattice Boltzmann equation, boudary condistions, bounce-back rule, Navier-Stokes equation
(72 pages, 2002)

39. R. Korn
Elementare Finanzmathematik
Keywords: Finanzmathematik, Aktien, Optionen, Portfolio-Optimierung, Börse, Lehrerweiterbildung, Mathematikunterricht
(98 pages, 2002)

40. J. Kallrath, M. C. Müller, S. Nickel
Batch Presorting Problems: Models and Complexity Results
Keywords: Complexity theory, Integer programming, Assigment, Logistics
(19 pages, 2002)

41. J. Linn
On the frame-invariant description of the phase space of the Folgar-Tucker equation
Key words: fiber orientation, Folgar-Tucker equation, injection molding
(5 pages, 2003)

42. T. Hanne, S. Nickel
A Multi-Objective Evolutionary Algorithm for Scheduling and Inspection Planning in Software Development Projects
Key words: multiple objective programming, project management and scheduling, software development, evolutionary algorithms, efficient set
(29 pages, 2003)

43. T. Bortfeld , K.-H. Küfer, M. Monz, A. Scherrer, C. Thieke, H. Trinkaus
Intensity-Modulated Radiotherapy - A Large Scale Multi-Criteria Programming Problem
Keywords: multiple criteria optimization, representative systems of Pareto solutions, adaptive triangulation, clustering and disaggregation techniques, visualization of Pareto solutions, medical physics, external beam radiotherapy planning, intensity modulated radiotherapy
(31 pages, 2003)

44. T. Halfmann, T. Wichmann
Overview of Symbolic Methods in Industrial Analog Circuit Design
Keywords: CAD, automated analog circuit design, symbolic analysis, computer algebra, behavioral modeling, system simulation, circuit sizing, macro modeling, differential-algebraic equations, index
(17 pages, 2003)

45. S. E. Mikhailov, J. Orlik
Asymptotic Homogenisation in Strength and Fatigue Durability Analysis of Composites
Keywords: multiscale structures, asymptotic homogenization, strength, fatigue, singularity, non-local conditions
(14 pages, 2003)

46. P. Domínguez-Marín, P. Hansen, N. Mladenovic , S. Nickel
Heuristic Procedures for Solving the Discrete Ordered Median Problem
Keywords: genetic algorithms, variable neighborhood search, discrete facility location
(31 pages, 2003)

47. N. Boland, P. Domínguez-Marín, S. Nickel, J. Puerto
Exact Procedures for Solving the Discrete Ordered Median Problem
Keywords: discrete location, Integer programming
(41 pages, 2003)

48. S. Feldmann, P. Lang
Padé-like reduction of stable discrete linear systems preserving their stability
Keywords: Discrete linear systems, model reduction, stability, Hankel matrix, Stein equation
(16 pages, 2003)

49. J. Kallrath, S. Nickel
A Polynomial Case of the Batch Presorting Problem
Keywords: batch presorting problem, online optimization, competetive analysis, polynomial algorithms, logistics
(17 pages, 2003)

50. T. Hanne, H. L. Trinkaus
knowCube for MCDM – Visual and Interactive Support for Multicriteria Decision Making
Key words: Multicriteria decision making, knowledge management, decision support systems, visual interfaces, interactive navigation, real-life applications.
(26 pages, 2003)

51. O. Iliev, V. Laptev
On Numerical Simulation of Flow Through Oil Filters
Keywords: oil filters, coupled flow in plain and porous media, Navier-Stokes, Brinkman, numerical simulation
(8 pages, 2003)

52. W. Dörfler, O. Iliev, D. Stoyanov, D. Vassileva
On a Multigrid Adaptive Refinement Solver for Saturated Non-Newtonian Flow in Porous Media
Keywords: Nonlinear multigrid, adaptive refinement, non-Newtonian flow in porous media
(17 pages, 2003)

53. S. Kruse
On the Pricing of Forward Starting Options under Stochastic Volatility
Keywords: Option pricing, forward starting options, Heston model, stochastic volatility, cliquet options
(11 pages, 2003)

54. O. Iliev, D. Stoyanov
Multigrid – adaptive local refinement solver for incompressible flows
Keywords: Navier-Stokes equations, incompressible flow, projection-type splitting, SIMPLE, multigrid methods, adaptive local refinement, lid-driven flow in a cavity
(37 pages, 2003)

55. V. Starikovicius
The multiphase flow and heat transfer in porous media
Keywords: Two-phase flow in porous media, various formulations, global pressure, multiphase mixture model, numerical simulation
(30 pages, 2003)

56. P. Lang, A. Sarishvili, A. Wirsen
Blocked neural networks for knowledge extraction in the software development process
Keywords: Blocked Neural Networks, Nonlinear Regression, Knowledge Extraction, Code Inspection
(21 pages, 2003)

57. H. Knaf, P. Lang, S. Zeiser
Diagnosis aiding in Regulation Thermography using Fuzzy Logic
Keywords: fuzzy logic,knowledge representation, expert system
(22 pages, 2003)

58. M. T. Melo, S. Nickel, F. Saldanha da Gama
Largescale models for dynamic multicommodity capacitated facility location
Keywords: supply chain management, strategic planning, dynamic location, modeling
(40 pages, 2003)

59. J. Orlik
Homogenization for contact problems with periodically rough surfaces
Keywords: asymptotic homogenization, contact problems
(28 pages, 2004)

60. A. Scherrer, K.-H. Küfer, M. Monz, F. Alonso, T. Bortfeld
IMRT planning on adaptive volume structures – a significant advance of computational complexity
Keywords: Intensity-modulated radiation therapy (IMRT), inverse treatment planning, adaptive volume structures, hierarchical clustering, local refinement, adaptive clustering, convex programming, mesh generation, multi-grid methods
(24 pages, 2004)

61. D. Kehrwald
Parallel lattice Boltzmann simulation of complex flows
Keywords: Lattice Boltzmann methods, parallel computing, microstructure simulation, virtual material design, pseudo-plastic fluids, liquid composite moulding
(12 pages, 2004)

62. O. Iliev, J. Linn, M. Moog, D. Niedziela, V. Starikovicius
On the Performance of Certain Iterative Solvers for Coupled Systems Arising in Discretization of Non-Newtonian Flow Equations

Keywords: Performance of iterative solvers, Preconditioners, Non-Newtonian flow
(17 pages, 2004)

63. R. Ciegis, O. Iliev, S. Rief, K. Steiner
On Modelling and Simulation of Different Regimes for Liquid Polymer Moulding
Keywords: Liquid Polymer Moulding, Modelling, Simulation, Infiltration, Front Propagation, non-Newtonian flow in porous media
(43 pages, 2004)

64. T. Hanne, H. Neu
Simulating Human Resources in Software Development Processes
Keywords: Human resource modeling, software process, productivity, human factors, learning curve
(14 pages, 2004)

65. O. Iliev, A. Mikelic, P. Popov
Fluid structure interaction problems in deformable porous media: Toward permeability of deformable porous media
Keywords: fluid-structure interaction, deformable porous media, upscaling, linear elasticity, stokes, finite elements
(28 pages, 2004)

66. F. Gaspar, O. Iliev, F. Lisbona, A. Naumovich, P. Vabishchevich
On numerical solution of 1-D poroelasticity equations in a multilayered domain
Keywords: poroelasticity, multilayered material, finite volume discretization, MAC type grid
(41 pages, 2004)

67. J. Ohser, K. Schladitz, K. Koch, M. Nöthe
Diffraction by image processing and its application in materials science
Keywords: porous microstructure, image analysis, random set, fast Fourier transform, power spectrum, Bartlett spectrum
(13 pages, 2004)

68. H. Neunzert
Mathematics as a Technology: Challenges for the next 10 Years
Keywords: applied mathematics, technology, modelling, simulation, visualization, optimization, glass processing, spinning processes, fiber-fluid interaction, trubulence effects, topological optimization, multicriteria optimization, Uncertainty and Risk, financial mathematics, Malliavin calculus, Monte-Carlo methods, virtual material design, filtration, bio-informatics, system biology
(29 pages, 2004)

69. R. Ewing, O. Iliev, R. Lazarov, A. Naumovich
On convergence of certain finite difference discretizations for 1D poroelasticity interface problems
Keywords: poroelasticity, multilayered material, finite volume discretizations, MAC type grid, error estimates
(26 pages,2004)

70. W. Dörfler, O. Iliev, D. Stoyanov, D. Vassileva
On Efficient Simulation of Non-Newtonian Flow in Saturated Porous Media with a Multigrid Adaptive Refinement Solver
Keywords: Nonlinear multigrid, adaptive renement, non-Newtonian in porous media
(25 pages, 2004)

71. J. Kalcsics, S. Nickel, M. Schröder
Towards a Unified Territory Design Approach – Applications, Algorithms and GIS Integration
Keywords: territory desgin, political districting, sales territory alignment, optimization algorithms, Geographical Information Systems
(40 pages, 2005)

72. K. Schladitz, S. Peters, D. Reinel-Bitzer, A. Wiegmann, J. Ohser
Design of acoustic trim based on geometric modeling and flow simulation for non-woven
Keywords: random system of fibers, Poisson line process, flow resistivity, acoustic absorption, Lattice-Boltzmann method, non-woven
(21 pages, 2005)

73. V. Rutka, A. Wiegmann
Explicit Jump Immersed Interface Method for virtual material design of the effective elastic moduli of composite materials
Keywords: virtual material design, explicit jump immersed interface method, effective elastic moduli, composite materials
(22 pages, 2005)

74. T. Hanne
Eine Übersicht zum Scheduling von Baustellen
Keywords: Projektplanung, Scheduling, Bauplanung, Bauindustrie
(32 pages, 2005)

75. J. Linn
The Folgar-Tucker Model as a Differetial Algebraic System for Fiber Orientation Calculation
Keywords: fiber orientation, Folgar–Tucker model, invariants, algebraic constraints, phase space, trace stability
(15 pages, 2005)

76. M. Speckert, K. Dreßler, H. Mauch, A. Lion, G. J. Wierda
Simulation eines neuartigen Prüfsystems für Achserprobungen durch MKS-Modellierung einschließlich Regelung
Keywords: virtual test rig, suspension testing, multibody simulation, modeling hexapod test rig, optimization of test rig configuration
(20 pages, 2005)

77. K.-H. Küfer, M. Monz, A. Scherrer, P. Süss, F. Alonso, A. S. A. Sultan, Th. Bortfeld, D. Craft, Chr. Thieke
Multicriteria optimization in intensity modulated radiotherapy planning
Keywords: multicriteria optimization, extreme solutions, real-time decision making, adaptive approximation schemes, clustering methods, IMRT planning, reverse engineering
(51 pages, 2005)

78. S. Amstutz, H. Andrä
A new algorithm for topology optimization using a level-set method
Keywords: shape optimization, topology optimization, topological sensitivity, level-set
(22 pages, 2005)

79. N. Ettrich
Generation of surface elevation models for urban drainage simulation
Keywords: Flooding, simulation, urban elevation models, laser scanning
(22 pages, 2005)

80. H. Andrä, J. Linn, I. Matei, I. Shklyar, K. Steiner, E. Teichmann
OPTCAST – Entwicklung adäquater Strukturoptimierungsverfahren für Gießereien Technischer Bericht (KURZFASSUNG)
Keywords: Topologieoptimierung, Level-Set-Methode, Gießprozesssimulation, Gießtechnische Restriktionen, CAE-Kette zur Strukturoptimierung
(77 pages, 2005)

81. N. Marheineke, R. Wegener
Fiber Dynamics in Turbulent Flows Part I: General Modeling Framework
Keywords: fiber-fluid interaction; Cosserat rod; turbulence modeling; Kolmogorov's energy spectrum; double-velocity correlations; differentiable Gaussian fields
(20 pages, 2005)

Part II: Specific Taylor Drag
Keywords: flexible fibers; k-ε turbulence model; fiber-turbulence interaction scales; air drag; random Gaussian aerodynamic force; white noise; stochastic differential equations; ARMA process
(18 pages, 2005)

82. C. H. Lampert, O. Wirjadi
An Optimal Non-Orthogonal Separation of the Anisotropic Gaussian Convolution Filter
Keywords: Anisotropic Gaussian filter, linear filtering, orientation space, nD image processing, separable filters
(25 pages, 2005)

83. H. Andrä, D. Stoyanov
Error indicators in the parallel finite element solver for linear elasticity DDFEM
Keywords: linear elasticity, finite element method, hierarchical shape functions, domain decom-position, parallel implementation, a posteriori error estimates
(21 pages, 2006)

84. M. Schröder, I. Solchenbach
Optimization of Transfer Quality in Regional Public Transit
Keywords: public transit, transfer quality, quadratic assignment problem
(16 pages, 2006)

85. A. Naumovich, F. J. Gaspar
On a multigrid solver for the three-dimensional Biot poroelasticity system in multilayered domains
Keywords: poroelasticity, interface problem, multigrid, operator-dependent prolongation
(11 pages, 2006)

86. S. Panda, R. Wegener, N. Marheineke
Slender Body Theory for the Dynamics of Curved Viscous Fibers
Keywords: curved viscous fibers; fluid dynamics; Navier-Stokes equations; free boundary value problem; asymptotic expansions; slender body theory
(14 pages, 2006)

87. E. Ivanov, H. Andrä, A. Kudryavtsev
Domain Decomposition Approach for Automatic Parallel Generation of Tetrahedral Grids
Key words: Grid Generation, Unstructured Grid, Delaunay Triangulation, Parallel Programming, Domain Decomposition, Load Balancing
(18 pages, 2006)

88. S. Tiwari, S. Antonov, D. Hietel, J. Kuhnert, R. Wegener
A Meshfree Method for Simulations of Interactions between Fluids and Flexible Structures
Key words: Meshfree Method, FPM, Fluid Structure Interaction, Sheet of Paper, Dynamical Coupling
(16 pages, 2006)

89. R. Ciegis , O. Iliev, V. Starikovicius, K. Steiner
Numerical Algorithms for Solving Problems of Multiphase Flows in Porous Media
Keywords: nonlinear algorithms, finite-volume method, software tools, porous media, flows
(16 pages, 2006)

90. D. Niedziela, O. Iliev, A. Latz
On 3D Numerical Simulations of Viscoelastic Fluids
Keywords: non-Newtonian fluids, anisotropic viscosity, integral constitutive equation
(18 pages, 2006)

91. A. Winterfeld
Application of general semi-infinite Programming to Lapidary Cutting Problems
Keywords: large scale optimization, nonlinear programming, general semi-infinite optimization, design centering, clustering
(26 pages, 2006)

92. J. Orlik, A. Ostrovska
Space-Time Finite Element Approximation and Numerical Solution of Hereditary Linear Viscoelasticity Problems
Keywords: hereditary viscoelasticity; kern approximation by interpolation; space-time finite element approximation, stability and a priori estimate
(24 pages, 2006)

93. V. Rutka, A. Wiegmann, H. Andrä
EJIIM for Calculation of effective Elastic Moduli in 3D Linear Elasticity
Keywords: Elliptic PDE, linear elasticity, irregular domain, finite differences, fast solvers, effective elastic moduli
(24 pages, 2006)

94. A. Wiegmann, A. Zemitis
EJ-HEAT: A Fast Explicit Jump Harmonic Averaging Solver for the Effective Heat Conductivity of Composite Materials
Keywords: Stationary heat equation, effective thermal conductivity, explicit jump, discontinuous coefficients, virtual material design, microstructure simulation, EJ-HEAT
(21 pages, 2006)

95. A. Naumovich
On a finite volume discretization of the three-dimensional Biot poroelasticity system in multilayered domains
Keywords: Biot poroelasticity system, interface problems, finite volume discretization, finite difference method
(21 pages, 2006)

96. M. Krekel, J. Wenzel
A unified approach to Credit Default Swaption and Constant Maturity Credit Default Swap valuation
Keywords: LIBOR market model, credit risk, Credit Default Swaption, Constant Maturity Credit Default Swap-method
(43 pages, 2006)

97. A. Dreyer
Interval Methods for Analog Circiuts
Keywords: interval arithmetic, analog circuits, tolerance analysis, parametric linear systems, frequency response, symbolic analysis, CAD, computer algebra
(36 pages, 2006)

98. N. Weigel, S. Weihe, G. Bitsch, K. Dreßler
Usage of Simulation for Design and Optimization of Testing
Keywords: Vehicle test rigs, MBS, control, hydraulics, testing philosophy
(14 pages, 2006)

99. H. Lang, G. Bitsch, K. Dreßler, M. Speckert
Comparison of the solutions of the elastic and elastoplastic boundary value problems
Keywords: Elastic BVP, elastoplastic BVP, variational inequalities, rate-independency, hysteresis, linear kinematic hardening, stop- and play-operator
(21 pages, 2006)

100. M. Speckert, K. Dreßler, H. Mauch
MBS Simulation of a hexapod based suspension test rig
Keywords: Test rig, MBS simulation, suspension, hydraulics, controlling, design optimization
(12 pages, 2006)

101. S. Azizi Sultan, K.-H. Küfer
A dynamic algorithm for beam orientations in multicriteria IMRT planning
Keywords: radiotherapy planning, beam orientation optimization, dynamic approach, evolutionary algorithm, global optimization
(14 pages, 2006)

102. T. Götz, A. Klar, N. Marheineke, R. Wegener
A Stochastic Model for the Fiber Lay-down Process in the Nonwoven Production
Keywords: fiber dynamics, stochastic Hamiltonian system, stochastic averaging
(17 pages, 2006)

103. Ph. Süss, K.-H. Küfer
Balancing control and simplicity: a variable aggregation method in intensity modulated radiation therapy planning
Keywords: IMRT planning, variable aggregation, clustering methods
(22 pages, 2006)

104. A. Beaudry, G. Laporte, T. Melo, S. Nickel
Dynamic transportation of patients in hospitals
Keywords: in-house hospital transportation, dial-a-ride, dynamic mode, tabu search
(37 pages, 2006)

105. Th. Hanne
Applying multiobjective evolutionary algorithms in industrial projects
Keywords: multiobjective evolutionary algorithms, discrete optimization, continuous optimization, electronic circuit design, semi-infinite programming, scheduling
(18 pages, 2006)

106. J. Franke, S. Halim
Wild bootstrap tests for comparing signals and images
Keywords: wild bootstrap test, texture classification, textile quality control, defect detection, kernel estimate, nonparametric regression
(13 pages, 2007)

107. Z. Drezner, S. Nickel
Solving the ordered one-median problem in the plane
Keywords: planar location, global optimization, ordered median, big triangle small triangle method, bounds, numerical experiments
(21 pages, 2007)

108. Th. Götz, A. Klar, A. Unterreiter, R. Wegener
Numerical evidance for the non-existing of solutions of the equations desribing rotational fiber spinning
Keywords: rotational fiber spinning, viscous fibers, boundary value problem, existence of solutions
(11 pages, 2007)

109. Ph. Süss, K.-H. Küfer
Smooth intensity maps and the Bortfeld-Boyer sequencer
Keywords: probabilistic analysis, intensity modulated radiotherapy treatment (IMRT), IMRT plan application, step-and-shoot sequencing
(8 pages, 2007)

110. E. Ivanov, O. Gluchshenko, H. Andrä, A. Kudryavtsev
Parallel software tool for decomposing and meshing of 3d structures
Keywords: a-priori domain decomposition, unstructured grid, Delaunay mesh generation
(14 pages, 2007)

111. O. Iliev, R. Lazarov, J. Willems
Numerical study of two-grid preconditioners for 1d elliptic problems with highly oscillating discontinuous coefficients
Keywords: two-grid algorithm, oscillating coefficients, preconditioner
(20 pages, 2007)

112. L. Bonilla, T. Götz, A. Klar, N. Marheineke, R. Wegener
Hydrodynamic limit of the Fokker-Planck-equation describing fiber lay-down processes
Keywords: stochastic dierential equations, Fokker-Planck equation, asymptotic expansion, Ornstein-Uhlenbeck process
(17 pages, 2007)

113. S. Rief
Modeling and simulation of the pressing section of a paper machine
Keywords: paper machine, computational fluid dynamics, porous media
(41 pages, 2007)

114. R. Ciegis, O. Iliev, Z. Lakdawala
On parallel numerical algorithms for simulating industrial filtration problems
Keywords: Navier-Stokes-Brinkmann equations, finite volume discretization method, SIMPLE, parallel computing, data decomposition method
(24 pages, 2007)

115. N. Marheineke, R. Wegener
Dynamics of curved viscous fibers with surface tension
Keywords: Slender body theory, curved viscous bers with surface tension, free boundary value problem
(25 pages, 2007)

116. S. Feth, J. Franke, M. Speckert
Resampling-Methoden zur mse-Korrektur und Anwendungen in der Betriebsfestigkeit
Keywords: Weibull, Bootstrap, Maximum-Likelihood, Betriebsfestigkeit
(16 pages, 2007)

117. H. Knaf
Kernel Fisher discriminant functions – a concise and rigorous introduction
Keywords: wild bootstrap test, texture classification, textile quality control, defect detection, kernel estimate, nonparametric regression
(30 pages, 2007)

118. O. Iliev, I. Rybak
On numerical upscaling for flows in heterogeneous porous media

Keywords: numerical upscaling, heterogeneous porous media, single phase flow, Darcy's law, multiscale problem, effective permeability, multipoint flux approximation, anisotropy
(17 pages, 2007)

119. O. Iliev, I. Rybak
On approximation property of multipoint flux approximation method
Keywords: Multipoint flux approximation, finite volume method, elliptic equation, discontinuous tensor coefficients, anisotropy
(15 pages, 2007)

120. O. Iliev, I. Rybak, J. Willems
On upscaling heat conductivity for a class of industrial problems
Keywords: Multiscale problems, effective heat conductivity, numerical upscaling, domain decomposition
(21 pages, 2007)

121. R. Ewing, O. Iliev, R. Lazarov, I. Rybak
On two-level preconditioners for flow in porous media
Keywords: Multiscale problem, Darcy's law, single phase flow, anisotropic heterogeneous porous media, numerical upscaling, multigrid, domain decomposition, efficient preconditioner
(18 pages, 2007)

122. M. Brickenstein, A. Dreyer
POLYBORI: A Gröbner basis framework for Boolean polynomials
Keywords: Gröbner basis, formal verification, Boolean polynomials, algebraic cryptoanalysis, satisfiability
(23 pages, 2007)

123. O. Wirjadi
Survey of 3d image segmentation methods
Keywords: image processing, 3d, image segmentation, binarization
(20 pages, 2007)

124. S. Zeytun, A. Gupta
A Comparative Study of the Vasicek and the CIR Model of the Short Rate
Keywords: interest rates, Vasicek model, CIR-model, calibration, parameter estimation
(17 pages, 2007)

125. G. Hanselmann, A. Sarishvili
Heterogeneous redundancy in software quality prediction using a hybrid Bayesian approach
Keywords: reliability prediction, fault prediction, non-homogeneous poisson process, Bayesian model averaging
(17 pages, 2007)

126. V. Maag, M. Berger, A. Winterfeld, K.-H. Küfer
A novel non-linear approach to minimal area rectangular packing
Keywords: rectangular packing, non-overlapping constraints, non-linear optimization, regularization, relaxation
(18 pages, 2007)

127. M. Monz, K.-H. Küfer, T. Bortfeld, C. Thieke
Pareto navigation – systematic multi-criteria-based IMRT treatment plan determination
Keywords: convex, interactive multi-objective optimization, intensity modulated radiotherapy planning
(15 pages, 2007)

128. M. Krause, A. Scherrer
On the role of modeling parameters in IMRT plan optimization
Keywords: intensity-modulated radiotherapy (IMRT), inverse IMRT planning, convex optimization, sensitivity analysis, elasticity, modeling parameters, equivalent uniform dose (EUD)
(18 pages, 2007)

129. A. Wiegmann
Computation of the permeability of porous materials from their microstructure by FFF-Stokes
Keywords: permeability, numerical homogenization, fast Stokes solver
(24 pages, 2007)

130. T. Melo, S. Nickel, F. Saldanha da Gama
Facility Location and Supply Chain Management – A comprehensive review
Keywords: facility location, supply chain management, network design
(54 pages, 2007)

131. T. Hanne, T. Melo, S. Nickel
Bringing robustness to patient flow management through optimized patient transports in hospitals
Keywords: Dial-a-Ride problem, online problem, case study, tabu search, hospital logistics
(23 pages, 2007)

132. R. Ewing, O. Iliev, R. Lazarov, I. Rybak, J. Willems
An efficient approach for upscaling properties of composite materials with high contrast of coefficients
Keywords: effective heat conductivity, permeability of fractured porous media, numerical upscaling, fibrous insulation materials, metal foams
(16 pages, 2008)

133. S. Gelareh, S. Nickel
New approaches to hub location problems in public transport planning
Keywords: integer programming, hub location, transportation, decomposition, heuristic
(25 pages, 2008)

134. G. Thömmes, J. Becker, M. Junk, A. K. Vaikuntam, D. Kehrwald, A. Klar, K. Steiner, A. Wiegmann
A Lattice Boltzmann Method for immiscible multiphase flow simulations using the Level Set Method
Keywords: Lattice Boltzmann method, Level Set method, free surface, multiphase flow
(28 pages, 2008)

135. J. Orlik
Homogenization in elasto-plasticity
Keywords: multiscale structures, asymptotic homogenization, nonlinear energy
(40 pages, 2008)

136. J. Almquist, H. Schmidt, P. Lang, J. Deitmer, M. Jirstrand, D. Prätzel-Wolters, H. Becker
Determination of interaction between MCT1 and CAII via a mathematical and physiological approach
Keywords: mathematical modeling; model reduction; electrophysiology; pH-sensitive microelectrodes; proton antenna
(20 pages, 2008)

137. E. Savenkov, H. Andrä, O. Iliev
An analysis of one regularization approach for solution of pure Neumann problem
Keywords: pure Neumann problem, elasticity, regularization, finite element method, condition number
(27 pages, 2008)

138. O. Berman, J. Kalcsics, D. Krass, S. Nickel
The ordered gradual covering location problem on a network
Keywords: gradual covering, ordered median function, network location
(32 pages, 2008)

139. S. Gelareh, S. Nickel
Multi-period public transport design: A novel model and solution approaches
Keywords: Integer programming, hub location, public transport, multi-period planning, heuristics
(31 pages, 2008)

140. T. Melo, S. Nickel, F. Saldanha-da-Gama
Network design decisions in supply chain planning
Keywords: supply chain design, integer programming models, location models, heuristics
(20 pages, 2008)

141. C. Lautensack, A. Särkkä, J. Freitag, K. Schladitz
Anisotropy analysis of pressed point processes
Keywords: estimation of compression, isotropy test, nearest neighbour distance, orientation analysis, polar ice, Ripley's K function
(35 pages, 2008)

142. O. Iliev, R. Lazarov, J. Willems
A Graph-Laplacian approach for calculating the effective thermal conductivity of complicated fiber geometries
Keywords: graph laplacian, effective heat conductivity, numerical upscaling, fibrous materials
(14 pages, 2008)

143. J. Linn, T. Stephan, J. Carlsson, R. Bohlin
Fast simulation of quasistatic rod deformations for VR applications
Keywords: quasistatic deformations, geometrically exact rod models, variational formulation, energy minimization, finite differences, nonlinear conjugate gradients
(7 pages, 2008)

144. J. Linn, T. Stephan
Simulation of quasistatic deformations using discrete rod models
Keywords: quasistatic deformations, geometrically exact rod models, variational formulation, energy minimization, finite differences, nonlinear conjugate gradients
(9 pages, 2008)

145. J. Marburger, N. Marheineke, R. Pinnau
Adjoint based optimal control using mesh-less discretizations
Keywords: Mesh-less methods, particle methods, Eulerian-Lagrangian formulation, optimization strategies, adjoint method, hyperbolic equations
(14 pages, 2008

146. S. Desmettre, J. Gould, A. Szimayer
Own-company stockholding and work effort preferences of an unconstrained executive
Keywords: optimal portfolio choice, executive compensation
(33 pages, 2008)

147. M. Berger, M. Schröder, K.-H. Küfer
A constraint programming approach for the two-dimensional rectangular packing problem with orthogonal orientations
Keywords: rectangular packing, orthogonal orientations non-overlapping constraints, constraint propagation
(13 pages, 2008)

148. K. Schladitz, C. Redenbach, T. Sych, M. Godehardt
Microstructural characterisation of open foams using 3d images
Keywords: virtual material design, image analysis, open foams
(30 pages, 2008)

149. E. Fernández, J. Kalcsics, S. Nickel, R. Ríos-Mercado
A novel territory design model arising in the implementation of the WEEE-Directive
Keywords: heuristics, optimization, logistics, recycling
(28 pages, 2008)

150. H. Lang, J. Linn
Lagrangian field theory in space-time for geometrically exact Cosserat rods
Keywords: Cosserat rods, geometrically exact rods, small strain, large deformation, deformable bodies, Lagrangian field theory, variational calculus
(19 pages, 2009)

151. K. Dreßler, M. Speckert, R. Müller, Ch. Weber
Customer loads correlation in truck engineering
Keywords: Customer distribution, safety critical components, quantile estimation, Monte-Carlo methods
(11 pages, 2009)

152. H. Lang, K. Dreßler
An improved multiaxial stress-strain correction model for elastic FE postprocessing
Keywords: Jiang's model of elastoplasticity, stress-strain correction, parameter identification, automatic differentiation, least-squares optimization, Coleman-Li algorithm
(6 pages, 2009)

153. J. Kalcsics, S. Nickel, M. Schröder
A generic geometric approach to territory design and districting
Keywords: Territory design, districting, combinatorial optimization, heuristics, computational geometry
(32 pages, 2009)

154. Th. Fütterer, A. Klar, R. Wegener
An energy conserving numerical scheme for the dynamics of hyperelastic rods
Keywords: Cosserat rod, hyperealstic, energy conservation, finite differences
(16 pages, 2009)

155. A. Wiegmann, L. Cheng, E. Glatt, O. Iliev, S. Rief
Design of pleated filters by computer simulations
Keywords: Solid-gas separation, solid-liquid separation, pleated filter, design, simulation
(21 pages, 2009)

156. A. Klar, N. Marheineke, R. Wegener
Hierarchy of mathematical models for production processes of technical textiles
Keywords: Fiber-fluid interaction, slender-body theory, turbulence modeling, model reduction, stochastic differential equations, Fokker-Planck equation, asymptotic expansions, parameter identification
(21 pages, 2009)

157. E. Glatt, S. Rief, A. Wiegmann, M. Knefel, E. Wegenke
Structure and pressure drop of real and virtual metal wire meshes
Keywords: metal wire mesh, structure simulation, model calibration, CFD simulation, pressure loss
(7 pages, 2009)

158. S. Kruse, M. Müller
Pricing American call options under the assumption of stochastic dividends – An application of the Korn-Rogers model
Keywords: option pricing, American options, dividends, dividend discount model, Black-Scholes model
(22 pages, 2009)

159. H. Lang, J. Linn, M. Arnold
Multibody dynamics simulation of geometrically exact Cosserat rods
Keywords: flexible multibody dynamics, large deformations, finite rotations, constrained mechanical systems, structural dynamics
(20 pages, 2009)

160. P. Jung, S. Leyendecker, J. Linn, M. Ortiz
Discrete Lagrangian mechanics and geometrically exact Cosserat rods
Keywords: special Cosserat rods, Lagrangian mechanics, Noether's theorem, discrete mechanics, frame-indifference, holonomic constraints
(14 pages, 2009)

161. M. Burger, K. Dreßler, A. Marquardt, M. Speckert
Calculating invariant loads for system simulation in vehicle engineering
Keywords: iterative learning control, optimal control theory, differential algebraic equations (DAEs)
(18 pages, 2009)

162. M. Speckert, N. Ruf, K. Dreßler
Undesired drift of multibody models excited by measured accelerations or forces
Keywords: multibody simulation, full vehicle model, force-based simulation, drift due to noise
(19 pages, 2009)

163. A. Streit, K. Dreßler, M. Speckert, J. Lichter, T. Zenner, P. Bach
Anwendung statistischer Methoden zur Erstellung von Nutzungsprofilen für die Auslegung von Mobilbaggern
Keywords: Nutzungsvielfalt, Kundenbeanspruchung, Bemessungsgrundlagen
(13 pages, 2009)

164. I. Correia, S. Nickel, F. Saldanha-da-Gama
The capacitated single-allocation hub location problem revisited: A note on a classical formulation
Keywords: Capacitated Hub Location, MIP formulations
(10 pages, 2009)

165. F. Yaneva, T. Grebe, A. Scherrer
An alternative view on global radiotherapy optimization problems
Keywords: radiotherapy planning, path-connected sublevelsets, modified gradient projection method, improving and feasible directions
(14 pages, 2009)

166. J. I. Serna, M. Monz, K.-H. Küfer, C. Thieke
Trade-off bounds and their effect in multi-criteria IMRT planning
Keywords: trade-off bounds, multi-criteria optimization, IMRT, Pareto surface
(15 pages, 2009)

167. W. Arne, N. Marheineke, A. Meister, R. Wegener
Numerical analysis of Cosserat rod and string models for viscous jets in rotational spinning processes
Keywords: Rotational spinning process, curved viscous fibers, asymptotic Cosserat models, boundary value problem, existence of numerical solutions
(18 pages, 2009)

168. T. Melo, S. Nickel, F. Saldanha-da-Gama
An LP-rounding heuristic to solve a multi-period facility relocation problem
Keywords: supply chain design, heuristic, linear programming, rounding
(37 pages, 2009)

169. I. Correia, S. Nickel, F. Saldanha-da-Gama
Single-allocation hub location problems with capacity choices
Keywords: hub location, capacity decisions, MILP formulations
(27 pages, 2009)

170. S. Acar, K. Natcheva-Acar
A guide on the implementation of the Heath-Jarrow-Morton Two-Factor Gaussian Short Rate Model (HJM-G2++)
Keywords: short rate model, two factor Gaussian, G2++, option pricing, calibration
(30 pages, 2009)

171. A. Szimayer, G. Dimitroff, S. Lorenz
A parsimonious multi-asset Heston model: calibration and derivative pricing
Keywords: Heston model, multi-asset, option pricing, calibration, correlation
(28 pages, 2009)

172. N. Marheineke, R. Wegener
Modeling and validation of a stochastic drag for fibers in turbulent flows
Keywords: fiber-fluid interactions, long slender fibers, turbulence modelling, aerodynamic drag, dimensional analysis, data interpolation, stochastic partial differential algebraic equation, numerical simulations, experimental validations
(19 pages, 2009)

173. S. Nickel, M. Schröder, J. Steeg
Planning for home health care services
Keywords: home health care, route planning, metaheuristics, constraint programming
(23 pages, 2009)

174. G. Dimitroff, A. Szimayer, A. Wagner
Quanto option pricing in the parsimonious Heston model
Keywords: Heston model, multi asset, quanto options, option pricing
(14 pages, 2009) 174. G. Dimitroff, A. Szimayer, A. Wagner

175. S. Herkt, K. Dreßler, R. Pinnau
Model reduction of nonlinear problems in structural mechanics
Keywords: flexible bodies, FEM, nonlinear model reduction, POD
(13 pages, 2009)

176. M. K. Ahmad, S. Didas, J. Iqbal
Using the Sharp Operator for edge detection and nonlinear diffusion
Keywords: maximal function, sharp function,image processing, edge detection, nonlinear diffusion
(17 pages, 2009)

177. M. Speckert, N. Ruf, K. Dreßler, R. Müller, C. Weber, S. Weihe
Ein neuer Ansatz zur Ermittlung von Erprobungslasten für sicherheitsrelevante Bauteile
Keywords: sicherheitsrelevante Bauteile, Kundenbeanspruchung, Festigkeitsverteilung, Ausfallwahrscheinlichkeit, Konfidenz, statistische Unsicherheit, Sicherheitsfaktoren
(16 pages, 2009)

178. J. Jegorovs
Wave based method: new applicability areas
Keywords: Elliptic boundary value problems, inhomogeneous Helmholtz type differential equations in bounded domains, numerical methods, wave based method, uniform B-splines
(10 pages, 2009)

179. H. Lang, M. Arnold
Numerical aspects in the dynamic simulation of geometrically exact rods
Keywords: Kirchhoff and Cosserat rods, geometrically exact rods, deformable bodies, multibody dynamics,artial differential algebraic equations, method of lines, time integration
(21 pages, 2009)

180. H. Lang
Comparison of quaternionic and rotation-free null space formalisms for multibody dynamics
Keywords: Parametrisation of rotations, differential-algebraic equations, multibody dynamics, constrained mechanical systems, Lagrangian mechanics
(40 pages, 2010)

181. S. Nickel, F. Saldanha-da-Gama, H.-P. Ziegler
Stochastic programming approaches for risk aware supply chain network design problems
Keywords: Supply Chain Management, multi-stage stochastic programming, financial decisions, risk
(37 pages, 2010)

182. P. Ruckdeschel, N. Horbenko
Robustness properties of estimators in generalized Pareto Models
Keywords: global robustness, local robustness, finite sample breakdown point, generalized Pareto distribution
(58 pages, 2010)

183. P. Jung, S. Leyendecker, J. Linn, M. Ortiz
A discrete mechanics approach to Cosserat rod theory – Part 1: static equilibria
Keywords: Special Cosserat rods; Lagrangian mechanics; Noether's theorem; discrete mechanics; frame-indifference; holonomic constraints; variational formulation
(35 pages, 2010)

184. R. Eymard, G. Printsypar
A proof of convergence of a finite volume scheme for modified steady Richards' equation describing transport processes in the pressing section of a paper machine
Keywords: flow in porous media, steady Richards' equation, finite volume methods, convergence of approximate solution
(14 pages, 2010)

185. P. Ruckdeschel
Optimally Robust Kalman Filtering
Keywords: robustness, Kalman Filter, innovation outlier, additive outlier
(42 pages, 2010)

186. S. Repke, N. Marheineke, R. Pinnau
On adjoint-based optimization of a free surface Stokes flow
Keywords: film casting process, thin films, free surface Stokes flow, optimal control, Lagrange formalism
(13 pages, 2010)

187. O. Iliev, R. Lazarov, J. Willems
Variational multiscale Finite Element Method for flows in highly porous media
Keywords: numerical upscaling, flow in heterogeneous porous media, Brinkman equations, Darcy's law, subgrid approximation, discontinuous Galerkin mixed FEM
(21 pages, 2010)

188. S. Desmettre, A. Szimayer
Work effort, consumption, and portfolio selection: When the occupational choice matters
Keywords: portfolio choice, work effort, consumption, occupational choice
(34 pages, 2010)

189. O. Iliev, Z. Lakdawala, V. Starikovicius
On a numerical subgrid upscaling algorithm for Stokes-Brinkman equations
Keywords: Stokes-Brinkman equations, subgrid approach, multiscale problems, numerical upscaling
(27 pages, 2010)

190. A. Latz, J. Zausch, O. Iliev
Modeling of species and charge transport in Li-Ion Batteries based on non-equilibrium thermodynamics
Keywords: lithium-ion battery, battery modeling, electrochemical simulation, concentrated electrolyte, ion transport
(8 pages, 2010)

191. P. Popov, Y. Vutov, S. Margenov, O. Iliev
Finite volume discretization of equations describing nonlinear diffusion in Li-Ion batteries
Keywords: nonlinear diffusion, finite volume discretization, Newton method, Li-Ion batteries
(9 pages, 2010)

192. W. Arne, N. Marheineke, R. Wegener
Asymptotic transition from Cosserat rod to string models for curved viscous inertial jets
Keywords: rotational spinning processes; inertial and viscous-inertial fiber regimes; asymptotic limits; slender-body theory; boundary value problems
(23 pages, 2010)

193. L. Engelhardt, M. Burger, G. Bitsch
Real-time simulation of multibody-systems for on-board applications
Keywords: multibody system simulation, real-time simulation, on-board simulation, Rosenbrock methods
(10 pages, 2010)

194. M. Burger, M. Speckert, K. Dreßler
Optimal control methods for the calculation of invariant excitation signals for multibody systems
Keywords: optimal control, optimization, mbs simulation, invariant excitation
(9 pages, 2010)

195. A. Latz, J. Zausch
Thermodynamic consistent transport theory of Li-Ion batteries
Keywords: Li-Ion batteries, nonequilibrium thermodynamics, thermal transport, modeling
(18 pages, 2010)

196. S. Desmettre
Optimal investment for executive stockholders with exponential utility
Keywords: portfolio choice, executive stockholder, work effort, exponential utility
(24 pages, 2010)

197. W. Arne, N. Marheineke, J. Schnebele, R. Wegener
Fluid-fiber-interactions in rotational spinning process of glass wool production
Keywords: Rotational spinning process, viscous thermal jets, fluid-fiber-interactions, two-way coupling, slender-body theory, Cosserat rods, drag models, boundary value problem, continuation method
(20 pages, 2010)

198. A. Klar, J. Maringer, R. Wegener
A 3d model for fiber lay-down in nonwoven production processes
Keywords: fiber dynamics, Fokker-Planck equations, diffusion limits
(15 pages, 2010)

199. Ch. Erlwein, M. Müller
A regime-switching regression model for hedge funds
Keywords: switching regression model, Hedge funds, optimal parameter estimation, filtering
(26 pages, 2011)

200. M. Dalheimer
Power to the people – Das Stromnetz der Zukunft
Keywords: Smart Grid, Stromnetz, Erneuerbare Energien, Demand-Side Management
(27 pages, 2011)

201. D. Stahl, J. Hauth
PF-MPC: Particle Filter-Model Predictive Control
Keywords: Model Predictive Control, Particle Filter, CSTR, Inverted Pendulum, Nonlinear Systems, Sequential Monte Carlo
(40 pages, 2011)

202. G. Dimitroff, J. de Kock
Calibrating and completing the volatility cube in the SABR Model
Keywords: stochastic volatility, SABR, volatility cube, swaption
(12 pages, 2011)

203. J.-P. Kreiss, T. Zangmeister
Quantification of the effectiveness of a safety function in passenger vehicles on the basis of real-world accident data
Keywords: logistic regression, safety function, real-world accident data, statistical modeling
(23 pages, 2011)

204. P. Ruckdeschel, T. Sayer, A. Szimayer
Pricing American options in the Heston model: a close look on incorporating correlation
Keywords: Heston model, American options, moment matching, correlation, tree method
(30 pages, 2011)

205. H. Ackermann, H. Ewe, K.-H. Küfer, M. Schröder
Modeling profit sharing in combinatorial exchanges by network flows
Keywords: Algorithmic game theory, profit sharing, combinatorial exchange, network flows, budget balance, core
(17 pages, 2011)

206. O. Iliev, G. Printsypar, S. Rief
A one-dimensional model of the pressing section of a paper machine including dynamic capillary effects
Keywords: steady modified Richards' equation, finite volume method, dynamic capillary pressure, pressing section of a paper machine
(29 pages, 2011)

207. I. Vecchio, K. Schladitz, M. Godehardt, M. J. Heneka
Geometric characterization of particles in 3d with an application to technical cleanliness
Keywords: intrinsic volumes, isoperimetric shape factors, bounding box, elongation, geodesic distance, technical cleanliness
(21 pages, 2011)

208. M. Burger, K. Dreßler, M. Speckert
Invariant input loads for full vehicle multibody system simulation
Keywords: multibody systems, full-vehicle simulation, optimal control
(8 pages, 2011)

209. H. Lang, J. Linn, M. Arnold
Multibody dynamics simulation of geometrically exact Cosserat rods
Keywords: flexible multibody dynamics, large deformations, finite rotations, constrained mechanical systems, structural dynamics
(28 pages, 2011)

210. G. Printsypar, R. Ciegis
On convergence of a discrete problem describing transport processes in the pressing section of a paper machine including dynamic capillary effects: one-dimensional case
Keywords: saturated and unsaturated fluid flow in porous media, Richards' approach, dynamic capillary pressure, finite volume methods, convergence of approximate solution
(24 pages, 2011)

211. O. Iliev, G. Printsypar, S. Rief
A two-cimensional model of the pressing section of a paper machine including dynamic capillary effects
Keywords: two-phase flow in porous media, steady modified Richards' equation, finite volume method, dynamic capillary pressure, pressing section of a paper machine, multipoint flux approximation
(44 pages, 2012)

212. M. Buck, O. Iliev, H. Andrä
Multiscale finite element coarse spaces for the analysis of linear elastic composites
Keywords: linear elasticity, domain decomposition, multiscale finite elements, robust coarse spaces, rigid body modes, discontinuous coefficients
(31 pages, 2012)

213. A. Wagner
Residual demand modeling and application to electricity pricing
Keywords: residual demand modeling, renewable infeed, wind infeed, solar infeed, electricity demand, German power market, merit-order effect
(28 pages, 2012)

214. O. Iliev, A. Latz, J. Zausch, S. Zhang
An overview on the usage of some model reduction approaches for simulations of Li-ion transport in batteries
Keywords: Li-ion batteries, porous electrode model, model reduction
(21 pages, 2012)

215. C. Zémerli, A. Latz, H. Andrä
Constitutive models for static granular systems and focus to the Jiang-Liu hyperelastic law
Keywords: granular elasticity, constitutive modelling, non-linear finite element method
(33 pages, 2012)

216. T. Gornak, J. L. Guermond, O. Iliev, P. D. Minev
A direction splitting approach for incompressible Brinkmann flow
Keywords: unsteady Navier-Stokes-Brinkman equations, direction splitting algorithms, nuclear reactors safety simulations
(16 pages, 2012)

217. Y. Efendiev, O. Iliev, C. Kronsbein
Multilevel Monte Carlo methods using ensemble level mixed MsFEM for two-phase flow and transport simulations
Keywords: two phase flow in porous media, uncertainty quantification, multilevel Monte Carlo
(28 pages, 2012)

218. J. Linn, H. Lang, A. Tuganov
Geometrically exact Cosserat rods with Kelvin-Voigt type viscous damping
Keywords: geometrically exact rods, viscous damping, Kelvin-Voigt model, material damping parameters
(10 pages, 2012)

219. M. Schulze, S. Dietz, J. Linn, H. Lang, A. Tuganov
Integration of nonlinear models of flexible body deformation in Multibody System Dynamics
Keywords: multibody system dynamics, flexible structures, discrete Cosserat rods, wind turbine rotor blades
(10 pages, 2012)

220. C. Weischedel, A. Tuganov, T. Hermansson, J. Linn, M. Wardetzky
Construction of discrete shell models by geometric finite differences
Keywords: geometrically exact shells, discrete differential geometry, rotation-free Kirchhoff model, triangular meshes
(10 pages, 2012)

221. M. Taralov, V. Taralova, P. Popov, O. Iliev, A. Latz, J. Zausch
Report on Finite Element Simulations of Electrochemical Processes in Li-ion Batteries with Thermic Effects
Keywords: Li-ion battery, FEM for nonlinear problems, FEM for discontinuous solutions, Nonlinear diffusion, Nonlinear interface conditions
(40 pages, 2012)

Status quo: November 2012